Early Alterations of Hippocampal Neuronal Firing Induced by Abeta42

OXFORD UNIVERSITY PRESS | Cerebral Cortex

Early alterations of hippocampal neuronal firing induced by Abeta42

Journal:	*Cerebral Cortex*
Manuscript ID	CerCor-2016-01096.R1
Manuscript Type:	Original Articles
Date Submitted by the Author:	n/a
Complete List of Authors:	Gavello, Daniela; University of Torino, Department of Drug Science Calorio, Chiara; Universita degli Studi di Torino, Department of Drug Science and Technology Franchino, Claudio; University of Torino, Department of Drug Science Cesano, Federico; Universita degli Studi di Torino, Department of Chemistry Carabelli, Valentina; University of Torino, Department of Drug Science Carbone, Emilio; CNISM Research Unit, Department of Neuroscience MARCANTONI, Andrea; Universita degli Studi di Torino, Department of Drug Science and Technology; Universita degli Studi di Torino, Department of Drug Science and Technology
Keywords:	big conductance Ca2+ activated potassium (BK) channels, NMDA receptors, ryanodine receptors, spontaneous calcium transients, voltage gated calcium channels

Early alterations of hippocampal neuronal firing induced by Abeta42

Daniela Gavello, Chiara Calorio, Claudio Franchino, Federico Cesano*, Valentina Carabelli, Emilio Carbone, Andrea Marcantoni

Department of Drug Science and Technology, Torino University (Italy)

* Department of Chemistry Via Pietro Giuria 7 10125, Torino University (Italy)

Address correspondence to: Andrea Marcantoni, Department of Drug Science and Technology, Torino University, Corso Raffaello 30 10125 Torino, Italy. Telephone: +390116708312 Fax: +390116708498 Email: andrea.macantoni@unito.it

Running title: Neuronal dysfunctions induced by Abeta42 oligomers

Abstract

We studied the effect of Amyloid β 1-42 oligomers (Abeta42) on Ca^{2+} dependent excitability profile of hippocampal neurons. Abeta42 is one of the Amyloid beta peptides produced by the proteolytic processing of the amyloid precursor protein (APP) and participates in the initiating event triggering the progressive dismantling of synapses and neuronal circuits. Our experiments on cultured hippocampal network reveal that Abeta42 increases intracellular Ca^{2+} concentration by 46% and inhibits firing discharge by 19%. More precisely, Abeta42 differently regulates ryanodine (RyRs), NMDA receptors (NMDARs) and voltage gated calcium channels (VGCCs) by increasing Ca^{2+} release through RyRs and inhibiting Ca^{2+} influx through NMDARs and VGCCs. The overall increased intracellular Ca^{2+} concentration causes stimulation of K^+ current carried by big conductance Ca^{2+} activated potassium (BK) channels and hippocampal network firing inhibition. We conclude that Abeta42 alters neuronal function by means of at least four main targets: RyRs, NMDARs, VGCCs and BK channels. The development of selective modulators of these channels may in turn be useful for developing effective therapies that could enhance the quality of life of AD patients during the early onset of the pathology.

Keywords: big conductance Ca^{2+} activated potassium (BK) channels, NMDA receptors, ryanodine receptors, spontaneous calcium transients, voltage gated Ca^{2+} channels.

Introduction

Among the various hallmarks of Alzheimer's disease (AD), the activation process of the "amyloid-cascade" is one of the most studied. It assumes that the accumulation of oligomers of Amyloid Beta peptides (Abeta), produced by the proteolytic processing of the amyloid precursor protein (APP) is the initiating event that triggers the progressive dismantling of synapses, neuronal circuits and networks (Palop JJ and L Mucke 2010). However, so far there are not yet clear data regarding any possible Abeta-induced impairment of neuronal network excitability. Our previous results indicate that in Tg2576 mice neurons from lateral entorhinal cortex (LEC) (Marcantoni A et al. 2014) are characterized by early impairments of their excitable profile. Tg2576 mice harbor the human APP gene with the Swedish mutation and display age-dependent accumulation of Abeta peptides, like Abeta40, Abeta42, Abeta*56 and exhibit hyperphosphorylated tau (Hsiao K et al.

1996). The use of these mice does not therefore clarify if one or more Abeta peptides cause neuronal dysfunctions. These latter are generated by multiple interactions between Abeta oligomers and neurons that could occur by their direct binding to membrane receptors, interaction with membrane lipids leading to pore channels formation or changes of membrane properties (Benilova I et al. 2012). The manifold mechanisms of interplay between Abeta peptides and neurons are followed by variable effects on neurons and vary from synaptic plasticity impairment (Puzzo D et al. 2015) to spines and cells loss. Here we propose to focus on the effects of Amyloid β 1-42 oligomer (Abeta42), whose accumulation induces early and severe neuronal function impairments (Lambert MP et al. 1998; Ripoli C et al. 2013). There are however contrasting findings concerning the effect of Abeta42 on neuronal excitability and synaptic function. Recent evidences show that spontaneous firing of cultured neuronal network recorded by means of microelectrode arrays (MEAs) is depressed by Abeta42 (Charkhkar H et al. 2015), that in turn inhibits synaptic function (Ripoli C et al. 2013). Other evidences indicate that Abeta42 enhances neuronal excitability (Minkeviciene R et al. 2009; Puzzo D et al. 2009; Tamagnini F et al. 2015). All together these results suggest that the effect of Abeta42 strongly depends on its concentration and aggregation state (Palop JJ and L Mucke 2010), but they fail to clarify its mechanism of action. Likewise, the existence of a correlation between excitatory impairments and Ca^{2+} dysregulation induced by Abeta42 is still not completely understood. Ca^{2+} regulates many neuronal functions such as gene transcription, excitability and synaptic activity. It is generally accepted that during AD both the mechanisms of Ca^{2+} entry (Thibault O et al. 2012; Wang Y and MP Mattson 2013) and Ca^{2+} release (Stutzmann GE et al. 2004; Oules B et al. 2012) are altered. This is shown both in transgenic mice (Oules B et al. 2012; Chakroborty S et al. 2013) and in neurons treated with Abeta peptides (Mattson MP 2010) as well as Abeta42 (Lazzari C et al. 2014). Here we studied the effect of Abeta42 on the Ca^{2+} dependent excitatory profile of hippocampal neurons using MEAs extracellular recordings on neuronal circuits, intracellular patch clamp recordings and Ca^{2+} fluorescence imaging on single neurons. When maintained in primary culture, hippocampal neurons generate spontaneous bursts of action potentials (Gavello D et al. 2012; Allio A et al. 2015) that occur in synchrony with phasic periods of Ca^{2+} entry (Murphy TH et al. 1992). These

neurons are in fact connected by synaptic contacts morphologically and physiologically similar to those present in vivo and are useful to investigate the relationship between excitability and synaptic function. We found that pre-incubation of neurons with Abeta42 raises intracellular Ca^{2+} concentration and causes a paradoxical firing inhibition. We suggest that Abeta42 stimulates Ca^{2+} to be released through ryanodine receptors (RyRs) and inhibits Ca^{2+} influx through NMDA receptors (NMDARs) as well as through voltage gated calcium channels (VGCCs). The Abeta42-induced Ca^{2+} release activates presynaptic BK Ca^{2+} activated potassium channels and inhibits neuronal firing by mainly acting at presynaptic glutamatergic terminals.

Material and Methods

Abeta42 preparation

Abeta42 (Sigma-Aldrich, St. Louis, MO) was dissolved in 1% ammonium hydroxide solution and stored at -20°C at a concentration of 1 mM. Before neuronal administration Abeta42 was dissolved into the culture medium at the experimental concentration of 1 μM. For the aggregation protocol the peptide was stored 24 h at 4°C to obtain oligomers and 48 h at room temperature before incubation with neurons (Dahlgren KN et al. 2002; Tamagno E et al. 2006). Unless indicated otherwise, the results were always obtained by comparing control neurons treated with picrotoxin (100 μM) for 48 h vs neurons incubated for 48 h with Abeta42 together with picrotoxin.

AFM (Atomic Force Microscopy)

Measurements were performed in the intermittent-contact regime (tapping-mode AFM, pyramidal cantilever with a tip radius <6nm) by using a modified Nanosurf Easyscan2 AFM instrument, equipped with a 10 μm high-resolution scan head, shielded by an acoustically insulated enclosure and placed on an anti-vibration platform. Before analysis, sample solution containing Abeta42 oligomers or fibrils at a concentration of 1 μM were diluted to 100 nM and then dropped on freshly cleaved mica. Samples were AFM imaged as soon as supports become dry.

Cell culture

All experiments were performed in accordance with the guidelines established by the National Council on Animal Care and approved by the local Animal Care Committee of Turin University. Hippocampal neurons were obtained from c57bl6 mouse 18-day embryos. Hippocampus was

rapidly dissected under sterile conditions, kept in cold HBSS (4ºC) with high glucose, and then digested with papain (0.5 mg/ml) dissolved in HBSS plus DNAse (0.1 mg/ml) as previously described (Gavello D et al. 2012). Isolated cells were then plated at the final density of 1200 cells/mm^2 onto the MEA (previously coated with poly-DL-lysine and laminine). Cells were incubated with 1 % penicillin/streptomycin, 1 % glutamax, 2.5 % fetal bovine serum, 2 % B-27 supplemented neurobasal medium in a humidified 5 % CO_2 atmosphere at 37ºC. Each MEA dish was covered with a fluorinated ethylene-propylene membrane (ALA scientific, Westbury, NY, USA) to reduce medium evaporation and maintain sterility, thus allowing repeated recordings from the same chip. Recordings were carried out at DIV 18.

Patch clamp experiments

Patch electrodes, fabricated from thick borosilicate glasses (Hilgenberg, Mansifield, Germany), were pulled to a final resistance of 3-5 MΩ. Patch clamp recordings were performed in whole cell configuration using a Multiclamp 700-B amplifier connected to a Digidata 1440 and governed by the pClamp10 software (Axon Instruments, Molecular Devices Ltd, USA).

Experiments were performed at room temperature (22-24 °C) in whole cell configuration and acquired with sample frequency of 10 KHz (Baldelli P et al. 2002; Baldelli P et al. 2005). Analysis was performed with Clampfit software (Axon Instruments). Data are expressed as means ± S.E.M and statistical significance was calculated by using Student's t-test. Values of $p< 0.05$ were considered significant. Where indicated, analysis of variance (ANOVA) followed by Bonferroni post-hoc test was used and p values <0.05 were considered significant.

Current clamp

Neurons were clamped at -70 mV (V_h) and depolarized for 50ms by injecting 800 pA of current.

Voltage clamp

For Ca^{2+} current recording neurons were hold at -70 mV (V_h) and depolarized for 50ms at -10mV in order to maximally activate inward Ca^{2+} current. K^+ currents were recorded by depolarizing neurons from -70 to +80 mV for 400 ms. Where indicated the depolarizing step was preceded by stimuli of increased duration (from 10 to 90 ms) to -10 mV to open all available voltage-gated Ca^{2+} channels (Marcantoni A et al. 2010). AMPA dependent eEPSCs following spontaneous APs or

electrical stimulation were recorded by holding neurons at -70 mV (V_h). Presynaptic electrical stimuli were delivered through a glass pipette (1 µm tip diameter) filled with Tyrode's solution and placed in contact with the soma of presynaptic neuron in a loose-seal configuration. eEPSCs were filtered at half the acquisition rate with 8-pole low-pass Bessel filter. Recording with leak current >100 pA or series resistance >20 MΩ were discarded. Current pulses of 0.1 ms and variable amplitude (10–45 µA) were generated by an isolated pulse stimulator (model 2100; A-M Systems, Carlsburg, WA, USA).

MEA recordings

Multisite extracellular recordings from 60 electrodes were performed using the MEA-system, purchased from Multi-Channel Systems (Reutlingen, Germany). Data acquisition was controlled through MC_Rack software (Multi-Channel Systems Reutlingen, Germany), setting the threshold for spike detection at -30 µV and sampling at 10 kHz. Experiments were performed in a non-humidified incubator at 37°C and with 5% CO_2, without replacing the culture medium. Before starting the experiments, cells were allowed to stabilize in the non-humified incubator for 90 seconds; then the spontaneous activity was recorded for 2 minutes.

Culture medium was supplemented with picrotoxin (100µM, Sigma Aldrich) for inhibiting the GABAergic synaptic currents.

Analysis of MEA activity

Bursts analysis was performed using Neuroexplorer software (Nex Technologies, Littleton, MA, USA) after spike sorting operations. A burst consists of a group of spikes with decreasing amplitude, thus we set a threshold of at least 3 spikes and a minimum burst duration of 10 ms. We set interval algorithm specifications such as maximum interval to start burst (0.17 sec) and maximum interval to end burst (0.3 sec) recorded in 0.02 s bins (Gavello D et al. 2012). Burst analysis was performed by monitoring the following parameters: mean frequency, number of bursts and mean burst duration. Cross correlation probability values were obtained by means of Neuroexplorer software using ± 2 s and 5 ms bin size.

Data are expressed as means ± S.E.M and statistical significance was calculated by using Student's t-test. Values of $p< 0.05$ were considered significant. The number of experiments is referred to the number of MEA each of those consisted of 59 recording electrodes.

Calcium imaging

Hippocampal neurons plated on glass petri dishes were loaded with the fluorescent Ca^{2+} indicator Fura2-AM dye (3 μM) (Invitrogen, Molecular Probes, Oregon, USA) for 1 hour. The fluorescent dye was then washed, and extracellular solution containing picrotoxin (100 μM) was replaced into the petri dish. The inverted microscope used (Leica DMI3000B, Wetzlar, Germany) was equipped with a short-arc xenon gas discharge lamp (Ushio, Cypress, California, US). Alternating excitation wavelengths of 340 nm and 380 nm were obtained by a monochromator (Till Photonics, Grafelfing, Germany). The emitted fluorescence was measured at 500-530 nm. Images were projected onto a EMCCD camera (QuantEM:512SC, Photometrics, Tucson, Arizona, US) and stored every 200 ms. Spontaneous Ca^{2+} transients were recorded both in control condition and after incubation with Abeta42 using Metafluor software (Molecular Devices, California, USA) for data acquisition. The relative change in fluorescence ($\Delta F/F$) was measured considering the peak of Ca^{2+} transients. Data are expressed as means ± S.E.M and statistical significance was calculated by using Student's t-test. Values of $p< 0.05$ were considered significant.

Solutions and drugs

For voltage clamp recording of Ca^{2+} currents the external solution contained (in mM): 135 TEACl, $2CaCl_2$, 2 $MgCl_2$, 10 HEPES, 10 glucose (pH 7.4 with CsCl). The internal solution contained (in mM): 90 CsCl, 20 TEACl, 10 EGTA, 10 Glucose, 1 $MgCl_2$, 4 ATP, 0.5 GTP, 15 Phosphocreatine (pH 7.4 with CsOH). For Ca^{2+} current recording, 300 nM TTX (Tocris Bioscience, Bristol, UK), 1 mM kynurenic acid (Sigma Aldrich), 100 μM picrotoxin were added to extracellular solution.

When K^+ current recording, Tyrode's Standard solution was used as extracellular solution and the intracellular solution was the same used in current clamp experiments.

For current-clamp recording extracellular Tyrode's Standard solution contained (in mM) 2 $CaCl_2$, 130 NaCl, 2 $MgCl_2$, 10 Hepes, 10 glucose, 4 KCl (pH 7.4). The intracellular solution contained (in

mM): 135 gluconic acid (potassium salt: K-gluconate), 5 NaCl, 2 MgCl2, 10 HEPES, 0.5 EGTA, 2 ATP-Tris, 0.4 Tris-GTP.

Nifedipine and paxilline were used to block respectively L-type Ca^{2+} channels and BK channels (Marcantoni A et al. 2010) while apamine (200 nM) was used to inhibit SK channels (Vandael DH et al. 2012) All these compounds were purchased from Sigma Aldrich.

eEPSCs were recorded by perfusing postsynaptic neurons with Tyrode's Standard solution supplemented with D-(-)-2-amino-5-phosphonopentanoic acid (D-AP5; 50 µM),picrotoxin (100 µM) and CGP58845 (5 µM) (Tocris, Bristol, UK) to avoid contamination from NMDA dependent and GABAergic receptors activated currents. Action potential driven eEPSCs were recorded by adding Tetrodoxin (10 nM) to limit polysynaptic activity (Raffaelli G et al. 2004). The standard internal solution was (in mM): 20 Cs-MSO_3, 90 CsCl, 10 Hepes, 5 EGTA, 2 $MgCl_2$, 4 ATP (disodium salt), 15 Phosphocreatine (pH 7.4). Electrically stimulated eEPSCs were recorded by adding QX-314 (N-(2,6-dimethylphenyl carbamoylmethyl) triethylammonium bromide; 10mM; Tocris) into the internal solution to block post synaptic Na^+ currents.

For Ca^{2+} imaging experiments the extracellular solution contained (in mM): 130 NaCl, 4 KCl, 2 $CaCl_2$, 10 Glucose, 10 Hepes, 0.8 $MgCl_2$, 0.4 Glicine (pH 7.4).

Where indicated, 6,7-Dinitroquinoxalone-2,3-Dione (DNQX, 20µM, Sigma Aldrich) and dantrolene (10µM, Sigma Aldrich) were used for blocking respectively AMPA dependent synaptic currents and RyRs.

Results

Role of somatic action potential and neurotransmitter release in governing spontaneous firing of hippocampal network

As already observed (Bacci A et al. 1999; Arnold FJ et al. 2004; Gavello D et al. 2012) after 18 days in vitro (DIV), networks of cultured hippocampal neurons fire spontaneously (Fig. 1 a). TTX-sensitive Na^+ channels are critical for somatic action potential (AP) generation and their block by 0.3 µM TTX caused the complete inhibition of spontaneous firing (Fig.1 a, top). Glutamatergic synapses are crucial as well for governing spontaneous depolarizations (Arnold FJ et al. 2004). In particular the block of glutamate release through the administration of the selective P/Q Ca^{2+}

channels blocker ω-Agatoxin IV A (Fig.1 a, middle) completely inhibited spontaneous firing by preventing Ca^{2+} dependent neurotransmitter release. The selective blocker of glutamatergic AMPA receptors DNQX (20 μM) completely abolished hippocampal electrical activity as well (Fig.1 a, bottom). As previously observed (Arnold FJ et al. 2004), one hour after the block of GABAA receptors with picrotoxin (100 μM), the firing frequency of control neurons increased from 0.9±0.1 Hz to 2.5±0.2 Hz (n=9, *** p<0.001) and tend to decrease over time (Fig. 1 b, c). We focused on the effect of picrotoxin after 48 to 72h from its incubation observing the generation of more regular and synchronized bursts of APs (Fig. 1 c white vs grey panels). All together these results indicate that spontaneous network depolarizations depend on both somatic APs and neurotransmitter release that mainly involves postsynaptic AMPA and GABAergic receptors.

Abeta42 oligomers inhibit spontaneous firing of hippocampal network

Although it is already known that amyloid beta peptides impair glutamatergic synaptic functions (Palop JJ and L Mucke 2010), here we focused on the effects of Abeta42 on spontaneous firing mediated by the activation of excitatory synapses. We therefore incubated neurons with Abeta42 (1 μM) together with picrotoxin (Fig.1 d) and measured the firing activity after one to 72 hours. Similarly to what observed in control neurons, after one hour of incubation with Abeta42 together with picrotoxin, firing frequency increased from 1.2±0.1 Hz to 2.4±0.1 Hz (n=11, *** p<0.001) (Fig. 1 b), but after 48 and 72 h (Fig. 1 d, grey panels) it was significantly reduced by Abeta42 if compared to what observed in control neurons (* p<0.05). In particular, after 48h of incubation with Abeta42 and picrotoxin the firing frequency was on average 1.3±0.1Hz (n=11) while control neurons displayed an average firing frequency of 1.6±0.1 Hz (n=9). Further analysis revealed that after 48 hours of incubation with Abeta42 the intraburst firing frequency remained unaffected (Fig.1 e), while the number of bursts (Fig.1 f), bursts duration (Fig.1 g) and the cross correlation values (Fig.1 h) decreased significantly. All together these results suggest that Abeta42 decreases the firing activity in mature hippocampal network. We tested the possibility that the effect of Abeta42 oligomers depended on their concentration (Puzzo D et al. 2009; Lee L et al. 2013). We therefore reduced the concentration of Abeta42 to 200 nM and after 48 h of incubation we observed again a firing frequency inhibition from 1.6±0.1 Hz (n= 6) to 1.0±0.1 Hz (n= 9, *** p<0.001, not shown). In

order to understand if the effect of Abeta42 depended by its aggregation state (Lambert MP et al. 1998; Dahlgren KN et al. 2002), we further treated hippocampal neurons with Abeta42 previously stored for 48 h at 37°C (Dahlgren KN et al. 2002). Following this procedure we observed, through AFM, that Abeta42 (1 μM) assembled in fibrils of 1-2 μM length 5-14 nM thickness (see supplementary Fig. S1). MEA recordings showed that incubation with Abeta42 fibrils for 48 h did not inhibit firing frequency that was 2.2±0.4 Hz (n= 5) in control and 2.6±0.2 Hz (n= 4) in neurons incubated with Abeta42 fibrils, p= 0.4) (not shown). We thus confirmed that Abeta42 dependent firing inhibition is influenced by its aggregation state and is detectable during the early phase of its production, when Abeta42 form oligomers rather than fibrils (Palop JJ and L Mucke 2010). From here on we thus performed experiments using Abeta42 only in the oligomeric form as described in the methods section at a concentration of 1 μM. Under these conditions AFM microscopy revealed that Abeta42 oligomers were characterized by a globular shape of average diameter of 10-100 nm and height comprised between 2-4 nm (supplementary Fig.S1), in line with what recently proposed by others (Manassero G et al. 2016).

Abeta42 oligomers increase the amplitude of spontaneous Ca^{2+} transients by potentiating Ca^{2+}released from RyRs

Spontaneous intracellular Ca^{2+} oscillations occur regularly in primary cultured hippocampal neurons (Fig.2 a). Abeta42 increased their amplitude by 46%, without affecting their frequency and the basal intracellular Ca^{2+} concentration (Fig. 2 b). Average $\Delta F/F$ values increased from 1.26±0.11 (n= 39) in control neurons to 1.84±0.23 (n= 30) in neurons incubated with Abeta42 for 48 h (Fig. 2 c, * $p<0.05$). Being postulated the ability of Abeta42 to form Ca^{2+} permeable pores in the plasma membrane (Demuro A et al. 2011), we measured whether changes in membrane resistance (R_m) were detectable after incubation of neurons with Abeta42. To this purpose, we performed patch-clamp recordings by holding neurons at -70-mV and injecting 50 pA negative current (not shown). The degree of hyperpolarization was measured and the correspondent value of R_m calculated in control neurons (0.19±0.03 GΩ, n=16) was comparable with that obtained in the presence of Abeta42 (0.18±0.04, n=7). The Ca^{2+} transients are generated by Ca^{2+} influx through plasma membrane and Ca^{2+} released from intracellular stores when IP_3 and/or RyRs are activated.

Considering the relevance of RyRs in AD onset and progression (Oules B et al. 2012; Chakroborty S et al. 2013), we analyzed their contribution in the generation of spontaneous Ca^{2+} transients. As already observed in chick motoneurons (Wang S et al. 2009) here we found that in control neurons RyRs contribute to the generation of spontaneous Ca^{2+} transients (Fig.2 d), but they are scarcely involved in the regulation of firing activity (Cheong E et al. 2011) (Fig. 2 e). The selective RyRs negative allosteric modulator dantrolene (10 μM) reduced indeed the peak amplitude of spontaneous Ca^{2+} transients by 31.9±8.7% (n=8) (Fig. 2 f) without altering the firing frequency (Fig. 2 g) and increasing by 17.0±7.7% the cross correlation (Fig. 2 h). Dantrolene mediated inhibition of Ca^{2+} transients in neurons treated with Abeta42 for 48 h (Fig. 2 i, f) was significantly larger than in control conditions (54.0±5.6%, n=8, *p<0.05), while the firing frequency (Fig. 2 l, g) and the cross correlation (Fig. 2 h) values increased respectively by 13.3±5.5% (n=9) and 53.6± 14.8% (*** p<0.001) after 48 h of incubation with Abeta42. To finally test if RyRs are targeted by Abeta42, we measured the amount of Ca^{2+} released through RyRs by stimulating neurons with the RYRs agonist caffeine (10 mM) (see supplementary Fig. S2). We found that the average $\Delta F/F$ value was significantly (* p<0.05) higher in Abeta42 treated neurons (0.9±0.1, n=6) with respect to control (0.3±0.1, n=6). We then concluded that Abeta42 increases the amount of Ca^{2+} released through RyRs and that its inhibition counteracts the effects of Abeta42 on spontaneous Ca^{2+} transients, firing frequency and synchronization of neuronal hippocampal network.

Abeta42 oligomers inhibit spontaneous firing through BK channels activation

We hypothesized that Ca^{2+} activated potassium channels (IK_{Ca}) (Marrion NV and SJ Tavalin 1998) could be responsible for Abeta42 dependent inhibition of neuronal firing following the increased amplitude of spontaneous Ca^{2+} transients. We first focused on small conductance potassium channels (SK channels) (see supplementary Fig. S3) (Stocker M et al. 1999; Cheong E *et al.* 2011) observing that in control conditions the administration of the SK channels blocker apamin (200 nM) did not significantly change the firing frequency (1.5±0.1 Hz (n=6) in control vs 1.4±0.1 Hz (n=6) with apamin (p=0.16)), while the cross correlation value increased by 20.0±5.0%. We then concluded that in control conditions, SK channels are mainly involved in controlling network synchronization. When SK channels were blocked in neurons previously incubated with Abeta42

(supplementary Fig. S3), we observed that the overall firing frequency decreased from 1.2±0.2 Hz (n=6) to 1.0±0.2 Hz, (***p<0.001) while the cross correlation value was unaffected or slightly inhibited (-8.0±3.0%). We concluded that SK channels inhibition does not contribute to recover the physiological firing parameters impaired by Abeta42.

Big conductance (BK) channels are involved in controlling firing rate (Storm JF 1987) and synaptic function (Raffaelli G et al. 2004) of rat hippocampal neurons. They were blocked by paxilline (1 μM) (Marcantoni A et al. 2010; Zhou Y and CJ Lingle 2014), but the firing frequency of control neurons was unaffected or slightly inhibited (-8.8±4.3%, n=5) (Fig.3 a) and the cross correlation value remained unaltered (not shown). These results suggest that in control conditions BK channels are not primarily involved in governing spontaneous firing of hippocampal network. On the contrary, when neurons were incubated for 48 h with Abeta42 (Fig. 3 b), paxilline potentiated the firing frequency by 32.1±5.6 % (n= 6) (Fig. 3 c) without altering the cross correlation value (not shown). This result suggests that BK channels function is stimulated by Abeta42 and that they contribute to inhibit the spontaneous firing observed in hippocampal network. To test this hypothesis we performed patch clamp experiments in voltage clamp configuration (Fig. 3 d, e). The maximum amplitude of K^+ current measured in voltage clamp experiments by depolarizing neurons from -70 to +80 mV for 400 ms was comparable among control and Abeta42 treated neurons and equal to 3.5±0.4 nA (n= 12) in control versus 3.3±0.5 nA (n= 10) in the presence of Abeta42. Though, the effect of paxilline was significantly potentiated by Abeta42. In particular, 14.7±2.3 % (n= 12) of the total outward potassium current is carried by BK channels in control neurons (Fig. 3 f), while in neurons treated with Abeta42 the BK current contribution is significantly (* p<0.05) increased to 23.4±3.2 % (n= 10). When the depolarizing step was preceded by stimuli of increased duration (from 10 to 90 ms) to -10 mV to open all available voltage-gated Ca^{2+} channels (Marcantoni A et al. 2010) we did not measure any further increase of the outward current (see supplementary Fig S4) suggesting that BK channels are maximally activated even in the absence of the above mentioned pre-step protocol. All together these results suggest that Abeta42 stimulates the paxilline sensitive outward current carried by BK channels.

Presynaptic BK channels are upregulated by Abeta42

It is generally accepted that, in neurons, BK channels are distributed both at somatic and synaptic sites (Raffaelli G et al. 2004; Martire M et al. 2010). In order to understand if somatic BK channels are targeted by Abeta42, we tested if the increased intracellular Ca^{2+} concentration induced by Abeta42 could affect AP duration (Marcantoni A et al. 2014). We therefore performed whole cell current clamp recordings and measured the width of the first AP generated by injecting squared pulses of depolarizing currents (see Methods). In control neurons (Fig.3 g) paxilline widened APs and the half width increased from 1.8±0.3 ms to 2.0±0.3 ms (n=17, * p<0.05) similarly to what observed in neurons treated with Abeta42 (Fig.3 h) where the half width value increased from 1.6±0.2 ms to 1.9±0.3 ms (n=24, * p<0.05). We therefore concluded that somatic BK channels are not affected by Abeta42 and focused on synaptic BK channels. We first measured the spontaneous eEPSCs following AP generation (see Methods). Administration of DNQX (20 μM) together with picrotoxin completely blocked eEPSCs (not shown) thus suggesting that they are mainly mediated by AMPA receptor activation. In control neurons (Fig. 3 i), neither the amplitude (Fig. 3 l), nor the frequency (Fig. 3 m) of AMPA dependent eEPSCs were affected by paxilline. The average amplitude was respectively -12.8±0.2 pA in control and -12.4±0.2 pA with paxilline (n= 12, p= 0.14), while the inter event interval (IEI) was 147.6±3.3 ms and 155.7±4.5 ms with paxilline (p= 0.13). We then concluded that in physiological conditions, while BK channels contribute to AP duration, they are not involved in controlling the AMPA dependent glutamatergic synapses. In good agreement with the decreased firing activity induced by Abeta42 administration (Fig. 1 b-d), when we compared control neurons with those treated with Abeta42 (Fig. 3 n), the eEPSCs amplitude of these latter increased significantly to -21.7±0.6 pA (n= 10, Fig.3 o) and was not sensitive to the presence of paxilline (-21.1±0.6 pA, p= 0.48). IEI values were significantly higher as well (189.3±7.7 ms, Fig. 3 p) and with paxilline they decreased to 131.3±5.9 ms (***p<0.001). All together these results suggest that, being Abeta42 able to alter both IEI and amplitude of eEPSCs, it targets AMPA dependent glutamatergic synapses at pre and post synaptic sites. Being only the IEI values affected by the presence of paxilline, we concluded that presynaptic BK channels dependent current is stimulated by Abeta42.

Although in control neurons BK channels are not involved in controlling spontaneous firing (Fig. 3 a), we tested the hypothesis that these latter could be recruited when the amount of Ca^{2+} released by RyRs increased, thus determining glutamatergic AMPA dependent current inhibition. To this purpose we measured electrically evoked monosynaptic AMPA dependent glutamatergic EPSCs (eEPSCs) in control conditions and after administration of caffeine and paxilline. These two compounds were used for respectively stimulate Ca^{2+} release from RyRs and inhibit BK channels. We observed that activation of RyRs by caffeine inhibited eEPSCs by 64% (from 152.0±73.0 pA, n= 28 to 54.2± 23.9 pA, n= 8, * $p<0.05$ by ANOVA) (Fig.4 a, d). Because this effect was abolished by paxilline, we concluded that, when Ca^{2+} released by RyRs increases, it activates BK channels which in turn inhibit AMPA dependent eEPSCs. We next tested whether in control neurons the inhibition of RyRs and/or BK channels could affect AMPA dependent synaptic transmission. Monosynaptic eEPSCs were first measured in the presence of paxilline (Fig. 4 b, d) and their average amplitude (142.0±19.3 pA, n= 20) was comparable to control conditions, unlike to what observed in Abeta42 treated neurons (Fig. 4 c, d), where the average eEPSCs amplitude (177.8±18.6 pA, n= 28) was increased by paxilline to 291.7±70.6 pA (n= 10, * $p<0.05$). Dantrolene (Fig. 4 b, e) did not change the average eEPSCs amplitude measured in control neurons (145.6±21.0, n= 15), that instead increased to 368.3±70.4 pA (n= 11, * $p<0.05$) after incubation with Abeta42 (Fig. 4 c, e). Simultaneous administration of dantrolene together with paxilline did not alter significantly the amplitude of eEPSCs in control neurons (168.0±42.0 pA, n= 15, Fig. 4 b, e), but abolished the potentiating effect observed in Abeta42 treated neurons, making the average eEPSCs amplitude (141.2±37.2 pA, n= 6) comparable to that measured before RyRs and BK channels inhibition (Fig. 4 c, e). These results confirm that Abeta42 inhibits the amplitude of AMPA dependent eEPSCs by stimulating RyRs and BK channels function.

NMDA receptors are inhibited by Abeta42 oligomers

DNQX (20 μM) and TTX (0.3 μM) completely abolished spontaneous Ca^{2+} transients (Fig.5 a), suggesting that AMPA receptors (AMPARs) and voltage gated Na^{+} channels control Ca^{2+} oscillations by governing respectively synaptic and somatic dependent depolarizations. Alternatively to AMPARs, NMDA receptors (NMDARs) as well can be activated by glutamate

released at excitatory synapses and mediate Ca^{2+} entering into neurons. We therefore focused on the mechanisms of Ca^{2+} entry through NMDARs by measuring their contribution in the regulation of Ca^{2+} influx both in control (Fig. 5 a) and in the presence of Abeta42 (Fig.5 b). The selective NMDARs blocker APV (50 μM) inhibited Ca^{2+} transients amplitude in control neurons by 68.5±7.2 % and this effect was more pronounced (***p<0.001) than in Abeta42 treated neurons (47.7±4.2 % of inhibition) (Fig.5 c). We next tested the effect of APV on spontaneous firing observing that it was inhibited by 59.8±2.6 % (n= 5) in control neurons (Fig. 5 d, f).This effect was significantly (***p<0.001) reduced to 33.6±7.3 % (n= 4) in Abeta42 treated neurons (Fig. 5 e, f). Cross correlation analysis (Fig. 5 g) showed that APV increased network synchronization by 25.9±5.5 % in control neurons and that this effect was significantly (*** p<0.001) more pronounced in the presence of Abeta42 (89.7±12.8 %). All together these results suggest that Abeta42 inhibits NMDARs and that these latter are important for governing both spontaneous network depolarizations and Ca^{2+} oscillations.

Abeta42 inhibits Ca^{2+} entry through VGCCs

Together with NMDARs, voltage gated Ca^{2+} channels (VGCCs) regulate Ca^{2+} entry through plasma membrane (Alford S et al. 1993; Goussakov I et al. 2010). We found that when cadmium (200 μM) was added to extracellular medium together with APV, it completely abolished intracellular Ca^{2+} oscillations (Fig.6 a), suggesting that, in control neurons, VGCCs together with NMDARs are important for governing spontaneous Ca^{2+} transients. We therefore performed patch clamp experiments to verify whether Abeta42 affect VGCCs, by considering both L- and non-L-type channels known to be largely expressed in hippocampal neurons (Baldelli P et al. 2000; Baldelli P et al. 2002). In control neurons (Fig.6 b) after 11-14 DIV the total Ca^{2+} current at -10 mV in 2 mM Ca^{2+} was -692.8±80.5 pA (n= 24) (Fig. 6 c). Addition of 3 μM nifedipine reduced the peak current amplitude to -430.3±55.6 pA (Fig. 6 b, c) indicating that L-type Ca^{2+} channels (LTCCs) contribute to 38 % of total Ca^{2+} current (256.1±37.4 pA), while the remaining 62 % of total Ca^{2+} current is carried by non-LTCCs. In the presence of Abeta42 the amount of total Ca^{2+} current (Fig.6 d) significantly decreased to -284.5 ±40.0 pA (n=17, ***p<0.001). When LTCCs were blocked with nifedipine, the remaining Ca^{2+} current was -162.6±31.8 pA (Fig. 6 c, d). The contribution of LTCCs was slightly

but not significantly increased to 42.6 % and the remaining 57.4 % of the total Ca^{2+} current carried by non-LTCCs was comparable to that of control neurons. We then concluded that Abeta42 oligomers decreased the amplitude of Ca^{2+} current carried by VGCCs without altering the proportion between L and non-LTCCs.

Discussion

We studied the effects of APP derived protein Abeta42 on neuronal network excitability. Our results suggest that, after 48h of incubation, Abeta42 inhibits spontaneous firing and increases Ca^{2+} transients amplitude. We suggest that Abeta42 is responsible for remodeling intracellular Ca^{2+} homeostasis as a consequence of RyRs stimulation followed by NMDARs and VGCCs inhibition. All together these effects contribute to reduce the network excitability through BK channels activation and inhibition of AMPA dependent synaptic current. Physiological excitatory parameters are partially restored through the inhibition of RyRs or BK channels suggesting that their selective target could be useful for treating early symptoms of AD.

Inhibition of spontaneous firing by Abeta42

Our previous reports (Gavello D *et* al. 2012; Allio A et al. 2015) show that primary cultures of hippocampal neurons generate spontaneous bursts of APs recorded extracellularly by means of MEAs. Here we show that spontaneous firing depends on both somatic and synaptic excitability (Fig. 1 a). In particular, we clearly define the degree of importance of both glutamatergic and GABAergic synapses in governing network excitability and show that, while it is completely abolished by blocking glutamatergic AMPA receptors, it is only partially altered when GABAergic (Fig. 1 c) and NMDARs (Fig. 5 d) are inhibited. Here we focused on the role of glutamatergic AMPA-dependent synapses to regulate spontaneous firing. However, future experiments will be needed for clarify any specific effect induced by Abeta42 on the GABAergic counterpart.

It is already well established that in AD the mechanisms of synaptic transmission are impaired (Ye H et al. 2010; Chong SA et al. 2011), but recent reports suggest that intrinsic neuronal excitable properties are modified too (Marcantoni A et al. 2014; Tamagnini F et al. 2015).These effects are often contradictory and not well understood, probably because many causal agents that contribute to AD onset exist and many animal models have been proposed to be suitable for studying this

pathology. A great quantity of data comes from experiments on AD transgenic animals that exhibit Abeta accumulation (Marchetti C and H Marie 2011). Among various forms of Abeta oligomers, Abeta42 is considered particularly toxic for neurons (Lambert MP et al. 1998). Here we focus on its effects on both spontaneous network excitability and Ca^{2+} oscillations.

One of the major issues concerning the use of Abeta42 is represented by its tendency to aggregate during time (Dahlgren KN et al. 2002; Puzzo D et al. 2009) and to exert different effects depending on its concentration that in turn affects the aggregation process as well (Mucke L and DJ Selkoe 2012). We therefore identified the main structure and concentration of Abeta42 responsible for neuronal dysfunction. We suggest that Abeta42 oligomers, rather than fibrils, are the main responsible for neuronal dysfunction. This conclusion agrees with most of the data presented in literature, but contrasts with others (Minkeviciene R et al. 2009) which identify Abeta42 fibrils as the main cause of the increased neuronal excitability observed. Being our experimental conditions significantly different from those reported by Minkeviciene et al. (e.g. Abeta42 concentration and time of exposure), we concluded that these conflicting results cannot be compared and we do not exclude that high concentrations (100 μM) of fibrils of Abeta42 during shorter period of incubations (1 h) could increase neuronal excitability. Moreover, the Abeta42 dependent effects here described could be presumably influenced by the presence of other Abeta peptides such as Abeta40. These latter may in turn influence the Abeta aggregation process as already reported (Kuperstein I et al. 2010). Future experiments will be necessary to clarify this issue. Finally, new insights about the effects of Abeta42 are provided in this work by MEA recordings: we demonstrate that the spontaneous neuronal firing is inhibited (Fig. 1 b, d), as well as the number and the duration of bursts (Fig. 1 f, g). Burst activity is critical for neuronal function since during those prolonged excitatory periods, typical of mature networks, Ca^{2+} enters into neurons and regulates many neuronal activities as well as neurotransmitter release. Furthermore, we clearly show that Abeta42 inhibits network synchronization (Fig. 1 h), causing, in this way, the reduction of effectiveness of synaptic input (Marcantoni A et al. 2014).

ABeta42 oligomers stimulate spontaneous calcium transients by mainly targeting RYRs.

As already observed in different neurons (Murphy TH et al. 1992; van den Pol AN et al. 1992; Bacci A et al. 1999; Wang S et al. 2009) network of primary cultured hippocampal neurons generate spontaneous Ca^{2+} transients (Fig. 2 a) of longer duration than bursts of APs. Here we show that bursts of APs occur on average 10 folds faster than Ca^{2+} transients (hundred ms duration vs s), suggesting that several bursts of APs occur during one single Ca^{2+} transient. We also suggest that a correlation between Ca^{2+} transient amplitudes and firing frequency exists and the general rule is that by increasing the amplitude of Ca^{2+} transients the firing frequency is inhibited. Several studies demonstrate that Ca^{2+} dyshomeostasis is early observed in AD and it can contribute to generate synaptic dysfunction. We aimed at evaluating the effect of ABeta42 on spontaneous Ca^{2+} transients and how these could be correlated with altered neuronal network excitability. To this regard, it has been proposed that Abeta42 could create pores into the plasma membrane and that these latter could contribute to determine Ca^{2+} dyshomeostasis phenomena (Demuro A et al. 2011). Our experiments show that neither the basal intracellular Ca^{2+} concentration (Fig. 2 b), nor the R_m value are altered by Abeta42. Thus we can conclude that, in our experimental conditions, Abeta42 does not form Ca^{2+} permeable pores. Increasing evidences support the idea that RyRs activity is upregulated in AD, but most of the studies are limited to transgenic mice (Oules B et al. 2012; Chakroborty S et al. 2013) and only few reports propose an effect of Abeta42 on RyRs (Supnet C et al. 2006; Lazzari C et al. 2014). Here, by blocking RyRs with dantrolene (Fig. 2) and stimulating them with caffeine (supplementary Fig. S2) we clearly show their increased function induced by Abeta42. As already observed in thalamocortical neurons (Cheong E et al. 2011), we propose that under basal physiological conditions the spontaneous firing network is not affected by Ca^{2+} released through RyRs. On the other hand it is known that when the duration (Cheong E et al. 2011) or the frequency (Riquelme D et al. 2010) of electrical stimuli increases, the amount of Ca^{2+} released by RyRs increases as well and becomes involved in setting the neuronal firing frequency. Similarly to what above described, here we suggest that when ABeta42 targets RyRs the amount of intracellular Ca^{2+} concentration increases enough to inhibit firing network. To support this hypothesis, we finally demonstrate that dantrolene is able to reverse the inhibitory effects of Abeta42 on firing activity and synchronization of hippocampal

network. Currently, the precise effect of Abeta42 on RyRs is still to be elucidated. Future experiments are needed to characterize whether Abeta42 is responsible for the increased Ca^{2+} loading of intracellular stores or for the increased number and/or conductance of available RyRs. To this regard, it has been recently shown (Barucker C et al. 2014) that, already after 30 min of incubation, Abeta42 is found in the nucleus and interferes with gene transcription. We therefore cannot exclude the hypothesis that after 48-72 h of incubation Abeta42 could interfere with RyRs gene transcription process. It is worth noticing that here we do not consider the effect of Abeta42 on IP_3 receptors. Many reports suggest that during AD the amount of Ca^{2+} released through IP_3 receptors is increased as well (Stutzmann GE et al. 2004; Oules B et al. 2012; Chakroborty S et al. 2013), but other recent reports indicate that their function is inhibited by Abeta42 (Lazzari C et al. 2014). Despite these contrasting results, it is well accepted that Ca^{2+} released through IP_3 receptors concurs to the activation of RyRs and that dantrolene treatment suppresses Ca^{2+} release from both receptors (Chakroborty S et al. 2013) thus confirming the effectiveness of dantrolene during AD onset.

BK channels are targeted by Abeta42

Our data demonstrate that Abeta42, besides inhibiting neuronal firing and synchronization, increases the amplitude of intracellular Ca^{2+} oscillations, thus suggesting a possible involvement of Ca^{2+} activated potassium channels (IK_{Ca}). Two classes of IK_{Ca} with different affinity for Ca^{2+} exist. They are represented by Ca^{2+} dependent small conductance (SK) and voltage and Ca^{2+} dependent large conductance (BK) K^+ channels (Fakler B and JP Adelman 2008). The former govern firing rate, adaptation, regularity of APs firing. Their block prevents the repolarization at the end of the single AP, thus decreasing the number of Na^+ channels available for the next spike, increasing AP width and bringing neuron to a depolarizing block condition (Vandael DH et al. 2015). This mechanism could explain the inhibition of firing frequency and synchronism induced by apamin on spontaneous firing of hippocampal neurons treated with Abeta42 (Fig. S3), similarly to what observed in AD mice models where the synaptic function is altered by upregulation of SK channels (Chakroborty S et al. 2012). However, since SK channels inhibition does not contribute to recover the physiological firing parameters impaired by Abeta42, therefore it is reasonable to assume they

do not represent a promising target for restoring impaired neuronal function. We next focused on the role of BK channels, characterized by lower degree of affinity for Ca^{2+} with respect to SK, being activated by higher intracellular Ca^{2+} concentration (more than 10 μM) (Vandael DH et al. 2015). For these reasons, in neurons or neuronal like cells, BK channels are co-localized with the Ca^{2+} source mainly represented either by Ca^{2+} channels (Marrion NV and SJ Tavalin 1998; Marcantoni A et al. 2010; Vandael DH et al. 2010), or by RyRs as well (Chavis P et al. 1998; Beurg M et al. 2005). It is generally accepted that BK channels are located at both somatic and synaptic sites (Hu H et al. 2001) and are respectively important for controlling the AP shape (Storm JF 1987) and the neurotransmitter release (Raffaelli G et al. 2004; Martire M et al. 2010). Similarly to what already described (Hu H et al. 2001), here we show that in control neurons BK channels contribute little to the total K^+ activated current (Fig. 3 d) even when increased amount of Ca^{2+} enters into neurons (supplementary Fig. S4). We therefore conclude that they regulate the AP shape (Fig. 3 g) but are scarcely involved in controlling spontaneous firing of hippocampal network (Fig. 3 a) and do not regulate neurotransmitter release (Fig. 3 i, 4 b), unless RyRs are strongly activated (Fig.4 a). On the contrary, in the presence of Abeta42, the increased amount of intracellular Ca^{2+} concentration potentiates BK channels activation (Fig. 3 e, f) and this effect is specific for the presynaptic (Fig. 3 n, 4 c), but not somatic (Fig. 3 h) compartment. We in fact show that paxilline increases the frequency (Fig. 3 p), but not the amplitude of spontaneous eEPSCs following AP generation (Fig. 3 o) and increases the amplitude of electrically evocked eEPSCs (Fig. 4 e), while the AP duration is comparable to that measured in control neurons (Fig. 3 g, h). Further experiments will be necessary to understand the molecular mechanism responsible for BK channels activation induced by Abeta42 since we cannot exclude that the density and/or the conductance of these channels are increased. To this regard, a recent report (Donnelier J et al. 2015) suggests that Abeta42 does not increase the expression of the BK α subunit expression reinforcing the hypothesis of increased BK channels conductance. Finally, the experiments here discussed do not only demonstrate the activation of BK current by Abeta42, in good agreement with previous findings (Ye H et al. 2010). They also indicate the presence of a strong link between the increased amount of Ca^{2+} released by RyRs, the activation of BK channels and inhibition of the amplitude of glutamatergic AMPA

dependent current (Fig. 4 a). These overall effects could be responsible for decreasing the rate of glutamate release and in turn the rate of spontaneous firing of hippocampal network. It is noteworthy that while the frequency of eEPSCs in neurons treated with ABeta42 is significantly reduced when compared to control conditions, their amplitude is higher (Fig.3 l, o). We therefore conclude that presynaptic BK channels could be preferentially coupled with RyRs and that postsynaptic AMPA receptors function is upregulated by ABeta42, but the specific effects induced by Abea42 respectively at pre and post synaptic glutamatergic compartment are still to be investigated, as well as the molecular pathway that determines the increased amount of Ca^{2+} released by RyRs. Finally, we cannot also exclude that a coupling between IP_3 receptors and BK channels could exist, but, while these latter are mainly distributed at somatic region, RyRs prefer synaptic sites (Goussakov I et al. 2010; Chakroborty S et al. 2012) where BK channels are upregulated. All together these results strongly indicate BK channels as a target for treating early symptoms of AD.

NMDARs and VGCCs are inhibited by Abeta42

NMDARs are important for controlling spontaneous Ca^{2+} transients and it is well accepted that they are inhibited during aging (Thibault O et al. 2007) and in AD (Yu JT et al. 2009). This mechanism of Ca^{2+} influx is thought to be involved in governing neuronal plasticity, learning and memory processes (Malenka RC et al. 1988) that are known to be impaired in AD (LaFerla FM 2002). Our data add new insights about the effect of ABeta42 in the regulation of intracellular Ca^{2+} concentration by NMDARs. First we demonstrate that Ca^{2+} transients recorded in cultured hippocampal neurons depend by both somatic APs generation and activation of glutamatergic synapses (Fig. 5 a). We in fact show that TTX administration abolishes completely Ca^{2+} oscillations and the same is observed by blocking AMPA receptors through DNQX. Our data suggest that AMPA receptors are essential for spontaneous generation of Ca^{2+} transients while NMDA contribute only partially to this phenomenon and confirm what already observed in rat derived hippocampal neurons (Bacci A et al. 1999). The involvement of NMDA receptors in governing spontaneous firing of hippocampal network (Fig. 5 d) has been studied too. Our results show that their inhibition contributes only in part to the recovery of neuronal firing properties impaired by

Abeta42, by increasing network synchronization, but not firing frequency, thus suggesting that the effectiveness of therapies for AD treatment based on NMDA receptors blockers actually employed mainly depends on their ability to preserve the neuronal network synchronism. We finally observed that the effect of APV on Ca^{2+} transients and firing is less pronounced in the presence of Abeta42 (Fig. 5 b, c). Even if future experiments will be needed for clarifying this issue, all together these results suggest that NMDARs and the spontaneous firing activity of hippocampal networks are inhibited by Abeta42.

Hippocampal pyramidal neurons express high densities of L-type Ca^{2+} channels (LTCCs) in the cell body and proximal dendrites. They contribute to increase Ca^{2+} entry following NMDARs activation and together with NMDARs are involved in the control of Ca^{2+} influx and neuronal plasticity in hippocampus (Westenbroek RE et al. 1990). In addition, VGCCs are important to regulate the excitability of neurons (Bean BP 2007) or neuronal like cells (Marcantoni A et al. 2009; Marcantoni A et al. 2010; Vandael DH et al. 2015) Several reports indicate that their contribution to Ca^{2+} entry through plasma membrane increases during age when they are up-regulated (Thibault O et al. 2007; Yu JT et al. 2009). LTCCs upregulation has been frequently observed during AD (Wang Y and MP Mattson 2013), but opposing evidences suggest that they can be inhibited as well (Thibault O et al. 2012). This underlies the variability of effects on Ca^{2+} homeostasis observed in AD probably correlated with the multifactorial causes of the pathology together with different responses of the brain region of interest. Here we show their involvement in the spontaneous generation of Ca^{2+} transients (Fig. 6 a) and the inhibition of both L and non-LTCCs isoforms (Fig. 6 b - d) induced by Abeta42. In conclusion, the present work clarifies the effects of Abeta42 on neuronal function and, by focusing on the mechanisms that regulate Ca^{2+} oscillations, firing, synaptic function, correlates data from neuronal networks with those on isolated neurons. We suggest that Abeta42 increases the amplitude of Ca^{2+} transients, decreases the firing rate and network synchronization by mainly increasing RyRs and BK channels functions and inhibiting NMDARs and VGCCs (Fig. 6 e). The modulation of these targets would represent a promising strategy for early treatment of AD. We wish finally to point out that previous results obtained by our group (Marcantoni A et al. 2014). revealed that excitatory profile of neurons from lateral entorhinal

cortex is early altered during AD onset. These results indicate that sensory inputs involved in memory formation, including olfactory information processing conveyed by lateral entorhinal cortex to hippocampus, might be early compromised and suggest how new diagnostic methods for an early identification of AD should be addressed.

Acknowledgments

This work was supported by MIUR (Euro-Mediterranean PRES project to AM, PRIN 2010/2011 project 2010JFYFY2 to EC), local funds from University of Torino to AM and VC, Telethon Foundation (grant # GGP15110) to EC. The authors declare no conflict of interests.

References

Alford S, Frenguelli BG, Schofield JG, Collingridge GL. 1993. Characterization of Ca2+ signals induced in hippocampal CA1 neurones by the synaptic activation of NMDA receptors. The Journal of physiology 469:693-716.

Allio A, Calorio C, Franchino C, Gavello D, Carbone E, Marcantoni A. 2015. Bud extracts from Tilia tomentosa Moench inhibit hippocampal neuronal firing through GABA and benzodiazepine receptors activation. Journal of ethnopharmacology.

Arnold FJ, Hofmann F, Bengtson CP, Wittmann M, Vanhoutte P, Bading H. 2004. Microelectrode array recordings of cultured hippocampal networks reveal a simple model for transcription and protein synthesis-dependent plasticity. The Journal of physiology 564:3-19.

Bacci A, Verderio C, Pravettoni E, Matteoli M. 1999. Synaptic and intrinsic mechanisms shape synchronous oscillations in hippocampal neurons in culture. The European journal of neuroscience 11:389-397.

Baldelli P, Forni PE, Carbone E. 2000. BDNF, NT-3 and NGF induce distinct new Ca2+ channel synthesis in developing hippocampal neurons. The European journal of neuroscience 12:4017-4032.

Baldelli P, Hernandez-Guijo JM, Carabelli V, Carbone E. 2005. Brain-derived neurotrophic factor enhances GABA release probability and nonuniform distribution of N- and P/Q-type channels on release sites of hippocampal inhibitory synapses. The Journal of neuroscience : the official journal of the Society for Neuroscience 25:3358-3368.

Baldelli P, Novara M, Carabelli V, Hernandez-Guijo JM, Carbone E. 2002. BDNF up-regulates evoked GABAergic transmission in developing hippocampus by potentiating presynaptic N- and P/Q-type Ca2+ channels signalling. The European journal of neuroscience 16:2297-2310.

Baldelli P, Novara M, Carabelli V, Hernandez-Guijo JM, Carbone E. 2002. BDNF up-regulates evoked GABAergic transmission in developing hippocampus by potentiating presynaptic N- and P/Q-type Ca2+ channels signalling. The European journal of neuroscience 16:2297-2310.

Barucker C, Harmeier A, Weiske J, Fauler B, Albring KF, Prokop S, Hildebrand P, Lurz R, Heppner FL, Huber O, Multhaup G. 2014. Nuclear translocation uncovers the amyloid peptide Abeta42 as a regulator of gene transcription. The Journal of biological chemistry 289:20182-20191.

Bean BP. 2007. The action potential in mammalian central neurons. Nature reviews Neuroscience 8:451-465.

Benilova I, Karran E, De Strooper B. 2012. The toxic Abeta oligomer and Alzheimer's disease: an emperor in need of clothes. Nature neuroscience 15:349-357.

Beurg M, Hafidi A, Skinner LJ, Ruel J, Nouvian R, Henaff M, Puel JL, Aran JM, Dulon D. 2005. Ryanodine receptors and BK channels act as a presynaptic depressor of neurotransmission in cochlear inner hair cells. The European journal of neuroscience 22:1109-1119.

Chakroborty S, Briggs C, Miller MB, Goussakov I, Schneider C, Kim J, Wicks J, Richardson JC, Conklin V, Cameransi BG, Stutzmann GE. 2013. Stabilizing ER Ca2+ channel function as an early preventative strategy for Alzheimer's disease. PloS one 7:e52056.

Chakroborty S, Kim J, Schneider C, Jacobson C, Molgo J, Stutzmann GE. 2012. Early presynaptic and postsynaptic calcium signaling abnormalities mask underlying synaptic depression in presymptomatic Alzheimer's disease mice. The Journal of neuroscience : the official journal of the Society for Neuroscience 32:8341-8353.

Charkhkar H, Meyyappan S, Matveeva E, Moll JR, McHail DG, Peixoto N, Cliff RO, Pancrazio JJ. 2015. Amyloid beta modulation of neuronal network activity in vitro. Brain research 1629:1-9.

Chavis P, Ango F, Michel JM, Bockaert J, Fagni L. 1998. Modulation of big K+ channel activity by ryanodine receptors and L-type Ca2+ channels in neurons. The European journal of neuroscience 10:2322-2327.

Cheong E, Kim C, Choi BJ, Sun M, Shin HS. 2011. Thalamic ryanodine receptors are involved in controlling the tonic firing of thalamocortical neurons and inflammatory pain signal processing. In. J Neurosci United States: p 1213-1218.

Chong SA, Benilova I, Shaban H, De Strooper B, Devijver H, Moechars D, Eberle W, Bartic C, Van Leuven F, Callewaert G. 2011. Synaptic dysfunction in hippocampus of transgenic mouse models of Alzheimer's disease: a multi-electrode array study. Neurobiology of disease 44:284-291.

Dahlgren KN, Manelli AM, Stine WB, Jr., Baker LK, Krafft GA, LaDu MJ. 2002. Oligomeric and fibrillar species of amyloid-beta peptides differentially affect neuronal viability. The Journal of biological chemistry 277:32046-32053.

Demuro A, Smith M, Parker I. 2011. Single-channel Ca(2+) imaging implicates Abeta1-42 amyloid pores in Alzheimer's disease pathology. The Journal of cell biology 195:515-524.

Donnelier J, Braun ST, Dolzhanskaya N, Ahrendt E, Braun AP, Velinov M, Braun JE. 2015. Increased Expression of the Large Conductance, Calcium-Activated K+ (BK) Channel in Adult-Onset Neuronal Ceroid Lipofuscinosis. PloS one 10:e0125205.

Fakler B, Adelman JP. 2008. Control of K(Ca) channels by calcium nano/microdomains. Neuron 59:873-881.

Gavello D, Rojo-Ruiz J, Marcantoni A, Franchino C, Carbone E, Carabelli V. 2012. Leptin counteracts the hypoxia-induced inhibition of spontaneously firing hippocampal neurons: a microelectrode array study. PloS one 7:e41530.

Goussakov I, Miller MB, Stutzmann GE. 2010. NMDA-mediated Ca(2+) influx drives aberrant ryanodine receptor activation in dendrites of young Alzheimer's disease mice. The Journal of neuroscience : the official journal of the Society for Neuroscience 30:12128-12137.

Hsiao K, Chapman P, Nilsen S, Eckman C, Harigaya Y, Younkin S, Yang F, Cole G. 1996. Correlative memory deficits, Abeta elevation, and amyloid plaques in transgenic mice. Science (New York, NY) 274:99-102.

Hu H, Shao LR, Chavoshy S, Gu N, Trieb M, Behrens R, Laake P, Pongs O, Knaus HG, Ottersen OP, Storm JF. 2001. Presynaptic Ca2+-activated K+ channels in glutamatergic hippocampal terminals and their role in spike repolarization and regulation of transmitter release. The Journal of neuroscience : the official journal of the Society for Neuroscience 21:9585-9597.

Kuperstein I, Broersen K, Benilova I, Rozenski J, Jonckheere W, Debulpaep M, Vandersteen A, Segers-Nolten I, Van Der Werf K, Subramaniam V, Braeken D, Callewaert G, Bartic C, D'Hooge R, Martins IC, Rousseau F, Schymkowitz J, De Strooper B. 2010. Neurotoxicity of Alzheimer's disease Abeta peptides is induced by small changes in the Abeta42 to Abeta40 ratio. The EMBO journal 29:3408-3420.

LaFerla FM. 2002. Calcium dyshomeostasis and intracellular signalling in Alzheimer's disease. Nature reviews Neuroscience 3:862-872.

Lambert MP, Barlow AK, Chromy BA, Edwards C, Freed R, Liosatos M, Morgan TE, Rozovsky I, Trommer B, Viola KL, Wals P, Zhang C, Finch CE, Krafft GA, Klein WL. 1998. Diffusible, nonfibrillar ligands derived from Abeta1-42 are potent central nervous system neurotoxins. Proceedings of the National Academy of Sciences of the United States of America 95:6448-6453.

Lazzari C, Kipanyula MJ, Agostini M, Pozzan T, Fasolato C. 2014. Abeta42 oligomers selectively disrupt neuronal calcium release. Neurobiology of aging 36:877-885.

Lee L, Kosuri P, Arancio O. 2013. Picomolar amyloid-beta peptides enhance spontaneous astrocyte calcium transients. Journal of Alzheimer's disease : JAD 38:49-62.

Malenka RC, Kauer JA, Zucker RS, Nicoll RA. 1988. Postsynaptic calcium is sufficient for potentiation of hippocampal synaptic transmission. Science (New York, NY) 242:81-84.

Manassero G, Guglielmotto M, Zamfir R, Borghi R, Colombo L, Salmona M, Perry G, Odetti P, Arancio O, Tamagno E, Tabaton M. 2016. Beta-amyloid 1-42 monomers, but not oligomers, produce PHF-like conformation of Tau protein. Aging Cell 15:914-923.

Marcantoni A, Carabelli V, Vandael DH, Comunanza V, Carbone E. 2009. PDE type-4 inhibition increases L-type Ca(2+) currents, action potential firing, and quantal size of exocytosis in mouse chromaffin cells. Pflugers Archiv : European journal of physiology 457:1093-1110.

Marcantoni A, Raymond EF, Carbone E, Marie H. 2014. Firing properties of entorhinal cortex neurons and early alterations in an Alzheimer's disease transgenic model. Pflugers Archiv : European journal of physiology 466:1437-1450.

Marcantoni A, Vandael DH, Mahapatra S, Carabelli V, Sinnegger-Brauns MJ, Striessnig J, Carbone E. 2010. Loss of Cav1.3 channels reveals the critical role of L-type and BK channel coupling in pacemaking mouse adrenal chromaffin cells. The Journal of neuroscience : the official journal of the Society for Neuroscience 30:491-504.

Marchetti C, Marie H. 2011. Hippocampal synaptic plasticity in Alzheimer's disease: what have we learned so far from transgenic models? Reviews in the neurosciences 22:373-402.

Marrion NV, Tavalin SJ. 1998. Selective activation of Ca2+-activated K+ channels by co-localized Ca2+ channels in hippocampal neurons. Nature 395:900-905.

Martire M, Barrese V, D'Amico M, Iannotti FA, Pizzarelli R, Samengo I, Viggiano D, Ruth P, Cherubini E, Taglialatela M. 2010. Pre-synaptic BK channels selectively control glutamate versus GABA release from cortical and hippocampal nerve terminals. Journal of neurochemistry 115:411-422.

Mattson MP. 2010. ER calcium and Alzheimer's disease: in a state of flux. In. Sci Signal United States: p pe10.

Minkeviciene R, Rheims S, Dobszay MB, Zilberter M, Hartikainen J, Fulop L, Penke B, Zilberter Y, Harkany T, Pitkanen A, Tanila H. 2009. Amyloid beta-induced neuronal hyperexcitability triggers progressive epilepsy. The Journal of neuroscience : the official journal of the Society for Neuroscience 29:3453-3462.

Mucke L, Selkoe DJ. 2012. Neurotoxicity of amyloid beta-protein: synaptic and network dysfunction. Cold Spring Harbor perspectives in medicine 2:a006338.

Murphy TH, Blatter LA, Wier WG, Baraban JM. 1992. Spontaneous synchronous synaptic calcium transients in cultured cortical neurons. The Journal of neuroscience : the official journal of the Society for Neuroscience 12:4834-4845.

Oules B, Del Prete D, Greco B, Zhang X, Lauritzen I, Sevalle J, Moreno S, Paterlini-Brechot P, Trebak M, Checler F, Benfenati F, Chami M. 2012. Ryanodine receptor blockade reduces amyloid-beta load and memory impairments in Tg2576 mouse model of Alzheimer disease. In. J Neurosci United States: p 11820-11834.

Palop JJ, Mucke L. 2010. Amyloid-beta-induced neuronal dysfunction in Alzheimer's disease: from synapses toward neural networks. Nature neuroscience 13:812-818.

Puzzo D, Gulisano W, Arancio O, Palmeri A. 2015. The keystone of Alzheimer pathogenesis might be sought in Abeta physiology. Neuroscience 307:26-36.

Puzzo D, Privitera L, Leznik E, Fa M, Staniszewski A, Palmeri A, Arancio O. 2009. Picomolar amyloid-beta positively modulates synaptic plasticity and memory in hippocampus. The Journal of neuroscience : the official journal of the Society for Neuroscience 28:14537-14545.

Raffaelli G, Saviane C, Mohajerani MH, Pedarzani P, Cherubini E. 2004. BK potassium channels control transmitter release at CA3-CA3 synapses in the rat hippocampus. The Journal of physiology 557:147-157.

Ripoli C, Piacentini R, Riccardi E, Leone L, Li Puma DD, Bitan G, Grassi C. 2013. Effects of different amyloid beta-protein analogues on synaptic function. Neurobiology of aging 34:1032-1044.

Riquelme D, Alvarez A, Leal N, Adasme T, Espinoza I, Valdes JA, Troncoso N, Hartel S, Hidalgo J, Hidalgo C, Carrasco MA. 2010. High-frequency field stimulation of primary neurons enhances ryanodine receptor-mediated Ca2+ release and generates hydrogen peroxide, which jointly stimulate NF-kappaB activity. Antioxidants & redox signaling 14:1245-1259.

Stocker M, Krause M, Pedarzani P. 1999. An apamin-sensitive Ca2+-activated K+ current in hippocampal pyramidal neurons. Proceedings of the National Academy of Sciences of the United States of America 96:4662-4667.

Storm JF. 1987. Action potential repolarization and a fast after-hyperpolarization in rat hippocampal pyramidal cells. The Journal of physiology 385:733-759.

Stutzmann GE, Caccamo A, LaFerla FM, Parker I. 2004. Dysregulated IP3 signaling in cortical neurons of knock-in mice expressing an Alzheimer's-linked mutation in presenilin1 results in exaggerated Ca2+ signals and altered membrane excitability. In. J Neurosci United States: p 508-513.

Supnet C, Grant J, Kong H, Westaway D, Mayne M. 2006. Amyloid-beta-(1-42) increases ryanodine receptor-3 expression and function in neurons of TgCRND8 mice. The Journal of biological chemistry 281:38440-38447.

Tamagnini F, Scullion S, Brown JT, Randall AD. 2015. Intrinsic excitability changes induced by acute treatment of hippocampal CA1 pyramidal neurons with exogenous amyloid beta peptide. Hippocampus 25:786-797.

Tamagno E, Bardini P, Guglielmotto M, Danni O, Tabaton M. 2006. The various aggregation states of beta-amyloid 1-42 mediate different effects on oxidative stress, neurodegeneration, and BACE-1 expression. Free radical biology & medicine 41:202-212.

Thibault O, Gant JC, Landfield PW. 2007. Expansion of the calcium hypothesis of brain aging and Alzheimer's disease: minding the store. Aging Cell 6:307-317.

Thibault O, Pancani T, Landfield PW, Norris CM. 2012. Reduction in neuronal L-type calcium channel activity in a double knock-in mouse model of Alzheimer's disease. Biochimica et Biophysica Acta (BBA) - Molecular Basis of Disease 1822:546-549.

van den Pol AN, Finkbeiner SM, Cornell-Bell AH. 1992. Calcium excitability and oscillations in suprachiasmatic nucleus neurons and glia in vitro. The Journal of neuroscience : the official journal of the Society for Neuroscience 12:2648-2664.

Vandael DH, Marcantoni A, Carbone E. 2015. Cav1.3 Channels as Key Regulators of Neuron-Like Firings and Catecholamine Release in Chromaffin Cells. Current molecular pharmacology 8:149-161.

Vandael DH, Marcantoni A, Mahapatra S, Caro A, Ruth P, Zuccotti A, Knipper M, Carbone E. 2010. Ca(v)1.3 and BK channels for timing and regulating cell firing. Molecular neurobiology 42:185-198.

Vandael DH, Zuccotti A, Striessnig J, Carbone E. 2012. Ca(V)1.3-driven SK channel activation regulates pacemaking and spike frequency adaptation in mouse chromaffin cells. The Journal of neuroscience : the official journal of the Society for Neuroscience 32:16345-16359.

Wang S, Polo-Parada L, Landmesser LT. 2009. Characterization of rhythmic Ca2+ transients in early embryonic chick motoneurons: Ca2+ sources and effects of altered activation of transmitter receptors. The Journal of neuroscience : the official journal of the Society for Neuroscience 29:15232-15244.

Wang Y, Mattson MP. 2013. L-type Ca2+ currents at CA1 synapses, but not CA3 or dentate granule neuron synapses, are increased in 3xTgAD mice in an age-dependent manner. Neurobiology of aging 35:88-95.

Westenbroek RE, Ahlijanian MK, Catterall WA. 1990. Clustering of L-type Ca2+ channels at the base of major dendrites in hippocampal pyramidal neurons. Nature 347:281-284.

Ye H, Jalini S, Mylvaganam S, Carlen P. 2010. Activation of large-conductance Ca(2+)-activated K(+) channels depresses basal synaptic transmission in the hippocampal CA1 area in APP (swe/ind) TgCRND8 mice. Neurobiology of aging 31:591-604.

Yu JT, Chang RC, Tan L. 2009. Calcium dysregulation in Alzheimer's disease: from mechanisms to therapeutic opportunities. Progress in neurobiology 89:240-255.

Zhou Y, Lingle CJ. 2014. Paxilline inhibits BK channels by an almost exclusively closed-channel block mechanism. The Journal of general physiology 144:415-440.

Figure legends

Fig.1

a) Spontaneous hippocampal electrical activity measured by means of MEAs by one representative recording channel at 18 DIV after one hour of incubation with picrotoxin. *top*) Spontaneous hippocampal electrical activity depends on the availability of TTX-sensitive somatic Nav1 channels. *middle*) The block of glutamate release through administration of presynaptic Cav 2.1 channels blocker ω-Agatoxin IVA (2 μM) completely inhibits spontaneous firing by preventing Ca^{2+} dependent neurotransmitter release. *bottom*) The selective AMPA receptors inhibitor DNQX completely abolishes hippocampal electrical activity **b**) Time course of hippocampal network firing frequency recorded from 1 to 72 hours after incubation with picrotoxin alone (control, dark grey diamonds) and together with Abeta42 (1 μM) (light grey squares). After 48 and 72 hours of incubation with picrotoxin the firing frequency is significantly decreased by Abeta42. **c**) Selection of three representative recording traces from the same MEA showing neuronal spontaneous firing in control conditions at 18 DIV (white) and after exposure to picrotoxin (100 μM) for respectively 48 (light grey panel) and 72 h (dark grey panel). The two insets refer to the magnification of single bursts of action potentials. **d**) Three representative recording traces from the same MEA showing the inhibition of spontaneous firing by Abeta42 (1 μM). Neuronal firing was recorded at 18 DIV

before administration of Abeta42 and picrotoxin (white panel) and compared to that measured after 48h (light grey panel) and 72 h (dark grey panel) from administration of Abeta42 together with picrotoxin. After 48 h (light grey bar) the intraburst firing frequency remains unaffected (**e**) while both number of bursts (**f**), bursts duration (**g**) and cross correlation (**h**) decrease significantly with respect to controls (dark grey bar).

Fig.2

a) After 18 DIV hippocampal network generates spontaneous Ca^{2+} transients whose amplitude is significantly increased (**b**) after incubation for 48 hours with Abeta42. **c**) Bar graph summarizing the increased amplitude of Ca^{2+} transients induced Abeta42 (light grey bar) with respect to controls (dark grey bars). **d**) In control conditions, the inhibition of RyRs with dantrolene decreases the amplitude of Ca^{2+} transients. **e**) MEA recording showing that in control neurons spontaneous firing is not influenced by dantrolene. **f**) Bar graph comparing the more pronounced inhibition of Ca^{2+} transients amplitude induced by dantrolene on Abeta42 treated cells (light grey bar) with respect to control (dark grey bar). In neurons treated for 48h with Abeta42 the effect of dantrolene is potentiated. **g**) Bar graph showing that when neurons are exposed to Abeta42 for 48 h (light grey bar), dantrolene increases the firing frequency and **h**) cross correlation probability. These effects are more pronounced than that observed in control neurons (dark grey bar). **i**) In neurons treated for 48h with Abeta42 the effect of dantrolene on the amplitude of Ca^{2+} transients is potentiated with respect to control (d). **l**) MEA recording showing that in Abeta42 treated neurons dantrolene increases the frequency of spontaneous firing.

Fig. 3

a) Three representative channels from the same MEA showing that while spontaneous firing is not altered by paxilline (1 μM) in control neurons, it is increased (**b**) in those treated for 48 hours with Abeta42. **c**) Bar graph summarizing that firing frequency of cultured hippocampal network is unaffected or slightly inhibited by paxilline in control neurons (dark grey bar), while it is increased in Abeta42 treated neurons (light grey bar). **d**) Paxilline (light grey trace) inhibits the total outward K^+

current (black trace) in control. **e**) The inhibition of K^+ current induced by paxilline is potentiated after 48 hours of incubation with Abeta42. **f**) Bar graph summarizing the contribution of BK activated current with respect to the total amount of K^+ current activated in hippocampal neurons in control conditions (dark grey bar) and in presence of Abeta42 (light grey bar). **g**) Paxilline (light grey trace) broadens the action potential shape in control neurons (black trace). The effect is comparable to that measured in neurons incubated for 48h with Abeta42 (**h**). The dotted lines in g, h correspond to membrane potential of 0 mV. **i**) Representative recording of AMPA eEPSCs elicited by spontaneous APs in control conditions. Paxilline does not modify neither the amplitude (**l**) nor the frequency (**m**) of eEPSCs following AP generation. **n**) In neurons treated with Abeta42 paxilline does not alter eEPSCs amplitude (**o**) but decreases the inter event interval (IEI) (**p**).

Fig. 4

a) In control neurons, electrically evoked AMPA eEPSCs amplitude is significantly inhibited by caffeine (10mM) while paxilline abolishes this effect, **b**) Administration of paxilline and dantrolene simultaneously or separately does not change the average amplitude of eEPSCs measured in control neurons. **c**) After incubation with Abeta42 oligomers for 48h eEPSCs amplitude increases when paxilline or dantrolene are administered separately. This effect is abolished when the two compounds are administered together. **d**) Bar graphs comparing the average eEPSCs amplitude in control neurons (dark grey bars) with that measured in neurons incubated 48h with Abeta42 (light grey bars). The average eEPSCs amplitudes of the two populations are comparable and are inhibited by caffeine in control neurons. This effect is abolished by paxilline. In control neurons paxilline alone does not interfere with the average eEPSCs amplitude, which is increased in neurons previously incubated with Abeta42. **e**) Bar graphs summarizing the effect of dantrolene alone and together with paxilline in control neurons (dark grey bars) and in those incubated for 48h with Abeta42 (light grey bars). eEPSCs amplitude from control neurons are not affected by dantrolene administered alone or together with paxilline. Dantrolene potentiates the eEPSCs amplitude in neurons previously incubated with Abeta42. This potentiating effect induced by dantrolene is abolished by paxilline.

Fig.5

a) DNQX completely abolishes Ca^{2+} oscillations both in control conditions and in neurons treated with Abeta42 oligomers (**b**). NMDA receptors contribute to Ca^{2+} oscillations in control (**a**) where APV inhibits the peak of Ca^{2+} transients. This effect is reduced in neurons treated with Abeta42 (**b**). The inhibition of somatic action potentials with TTX abolishes the Ca^{2+} oscillations as well (**a**). **c**) Bar graph showing that Abeta42 (light grey bar) significantly reduces the effect of APV with respect to control (dark grey bar). **d**) APV inhibits spontaneous firing of hippocampal network. This effect is reduced by Abeta42 (**e**). **f**) Bar graph summarizing the inhibition of spontaneous firing frequency induced by APV in control (dark grey bar) and in neurons incubated with Abeta42. The inhibitory effect is significantly depressed by Abeta42. **g**) Bar graph summarizing the potentiating effect of APV on network synchronization measured by considering the cross correlation probability. Although APV inhibits the average firing frequency (f) it increases network synchronization more markedly in neurons treated with Abeta42 than in control.

Fig.6

a) In control neurons cadmium together with APV completely abolishes intracellular Ca^{2+} oscillations. **b**) In control neurons nifedipine (light grey trace) reduces by 38% the total Ca^{2+} current (black trace). **c**) Bar graph showing the almost proportional halving of total, non-L type and L-type Ca^{2+} currents induced by incubation of neurons with Abeta42 (light grey bars) when compared to control conditions (dark grey bars). **d**) Similarly to what observed in control neurons, nifedipine (light grey trace) inhibits by 43% the total Ca^{2+} current (black trace) after incubation with Abeta42. **e**) Chart summarizing the main results obtained: Abeta42 increases intracellular Ca^{2+} concentration of primary cultured hippocampal and inhibits neuronal network excitability by mainly increasing the amount of Ca^{2+} released through RyRs that in turn inhibits glutamatergic AMPA dependent synapses through activation of BK channels. Finally, a further contribution to firing inhibition is given by the decreased Ca^{2+} influx through NMDARs and VGCCs induced by Abeta42.

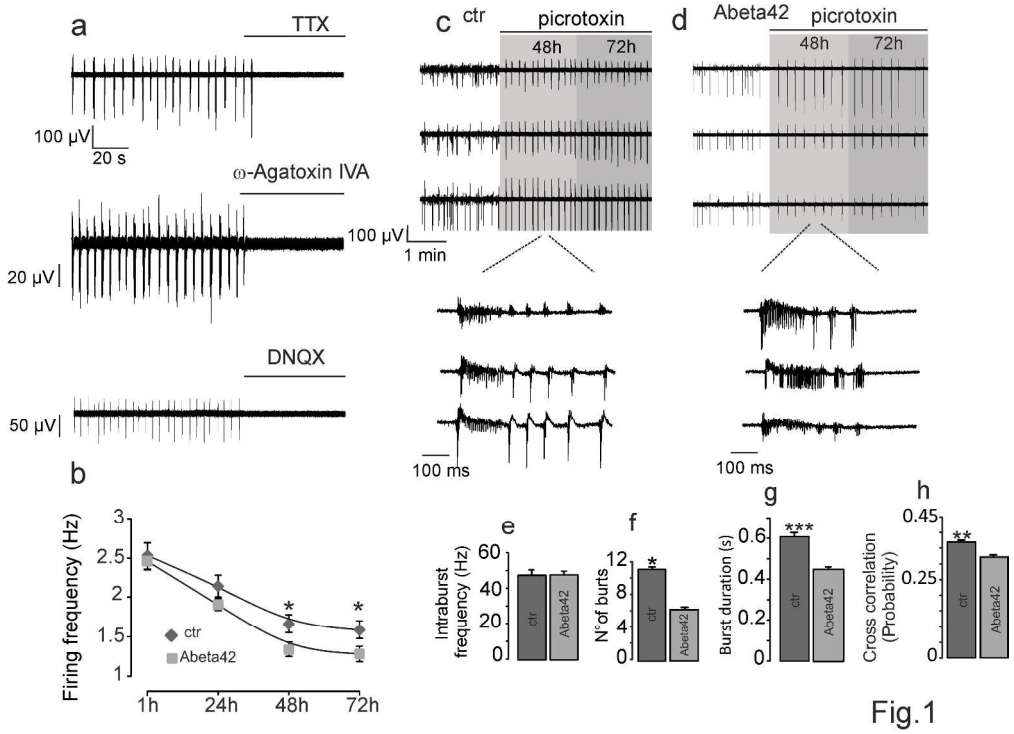

Fig.1

Fig.1

278x201mm (300 x 300 DPI)

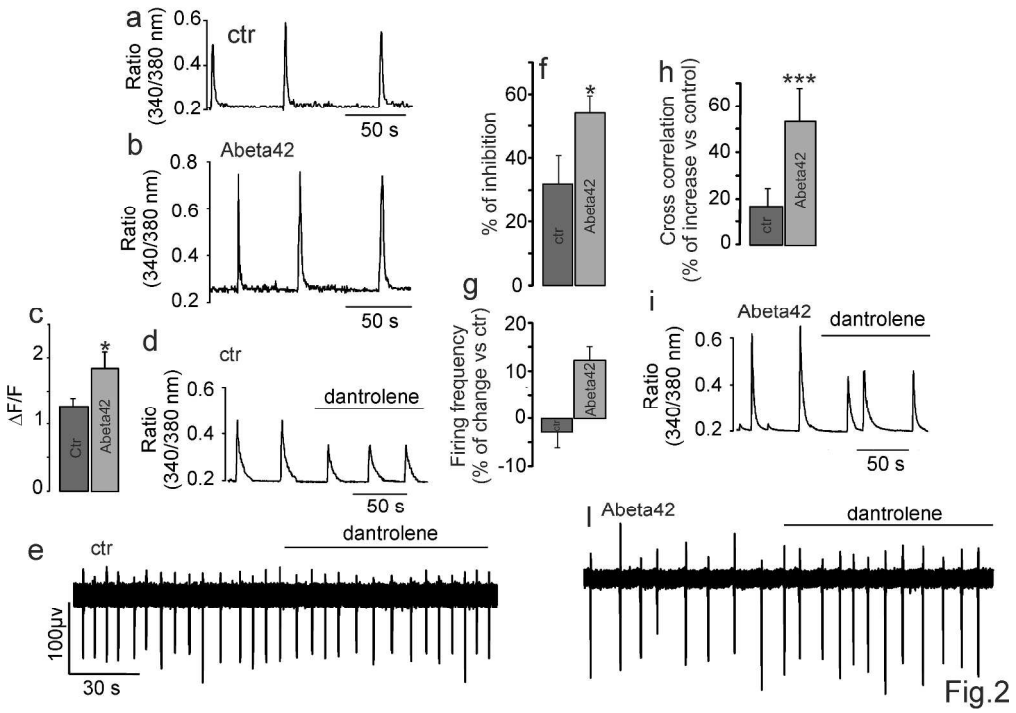

Fig.2

Fig.2

284x199mm (300 x 300 DPI)

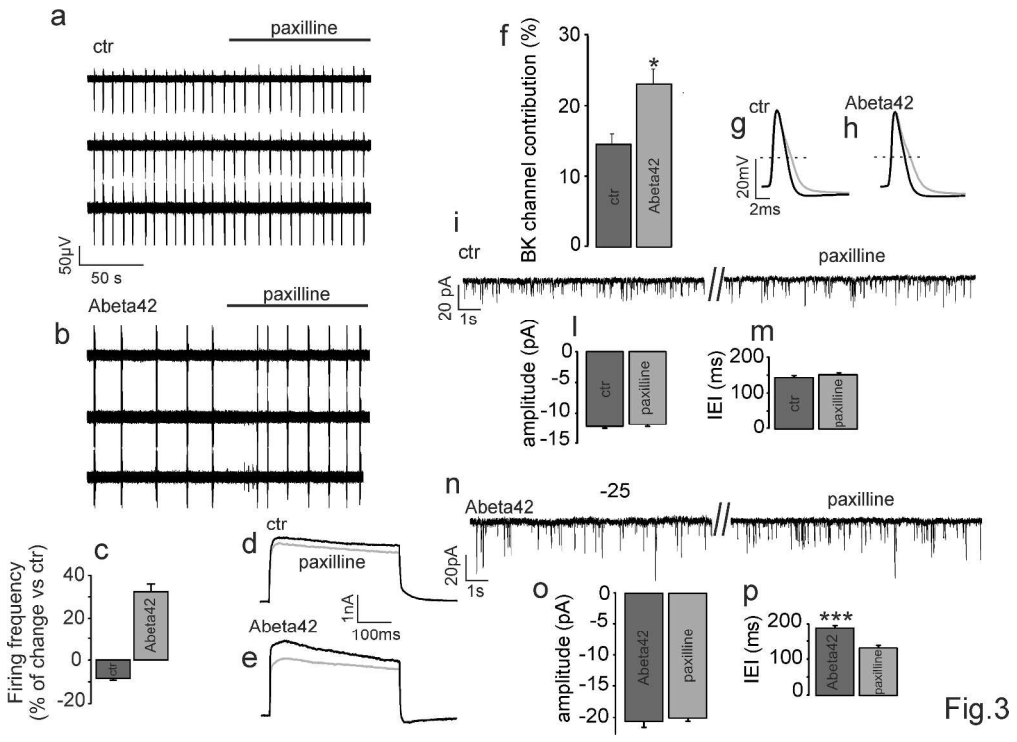

Fig.3

Fig.3

284x206mm (300 x 300 DPI)

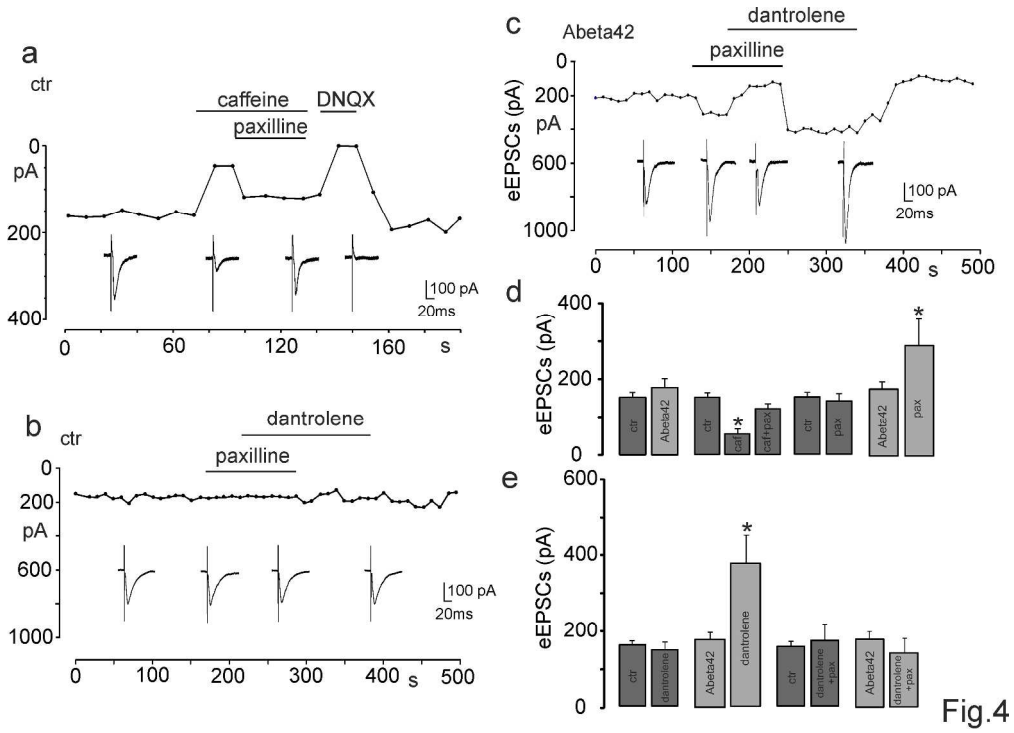

Fig.4

Fig.4

273x197mm (300 x 300 DPI)

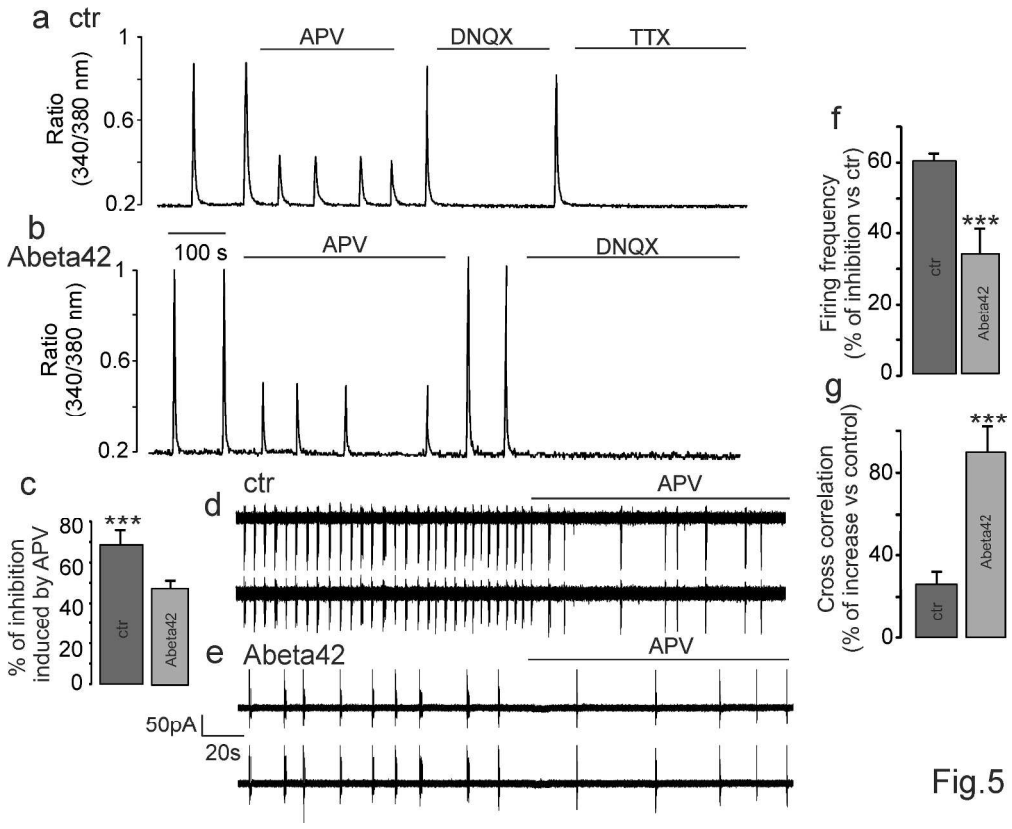

Fig.5

Fig.5

255x207mm (300 x 300 DPI)

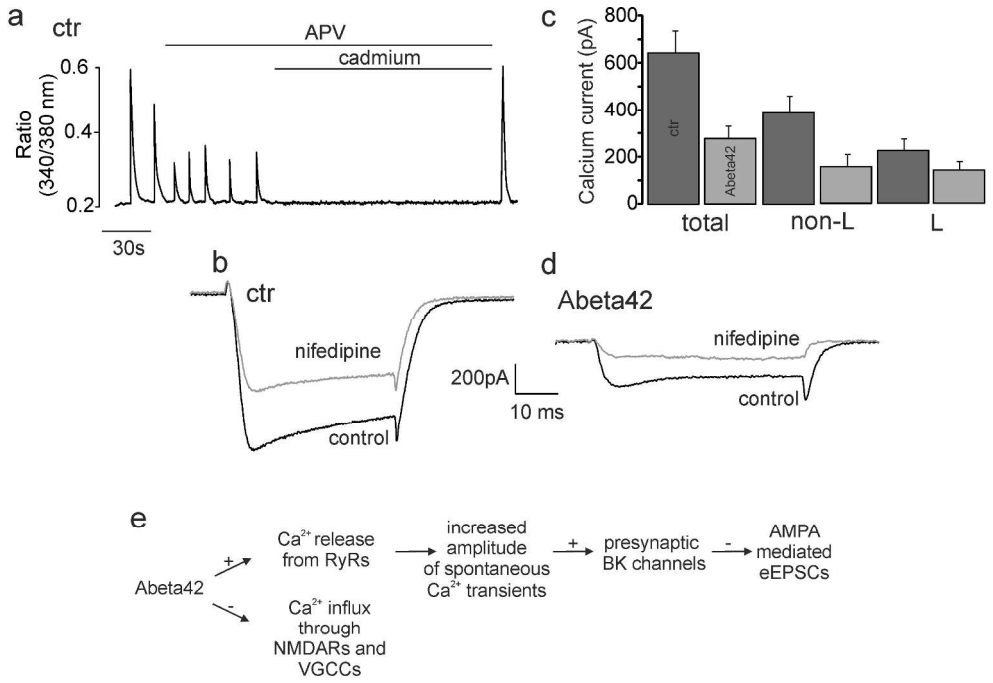

Fig.6

Fig.6

279x202mm (300 x 300 DPI)

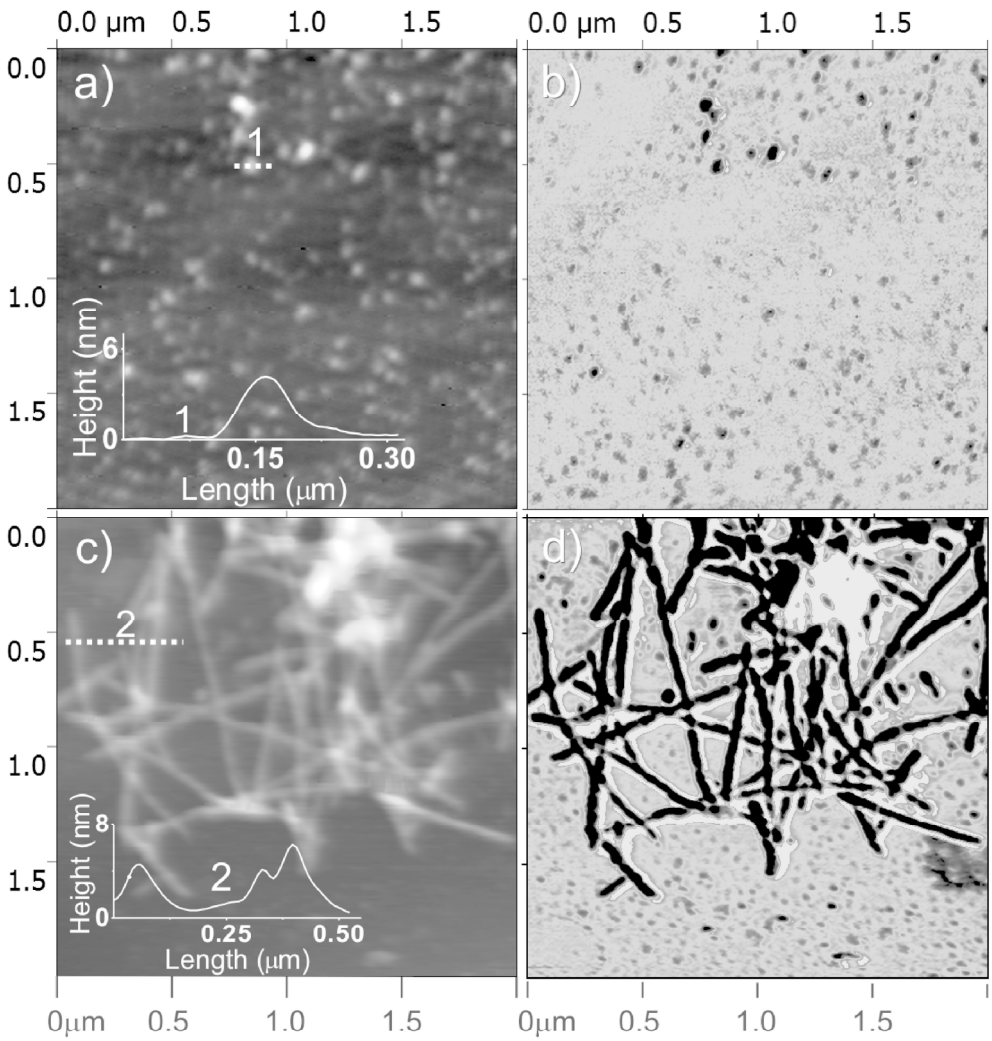

Fig. S1

Fig. S1

176x199mm (300 x 300 DPI)

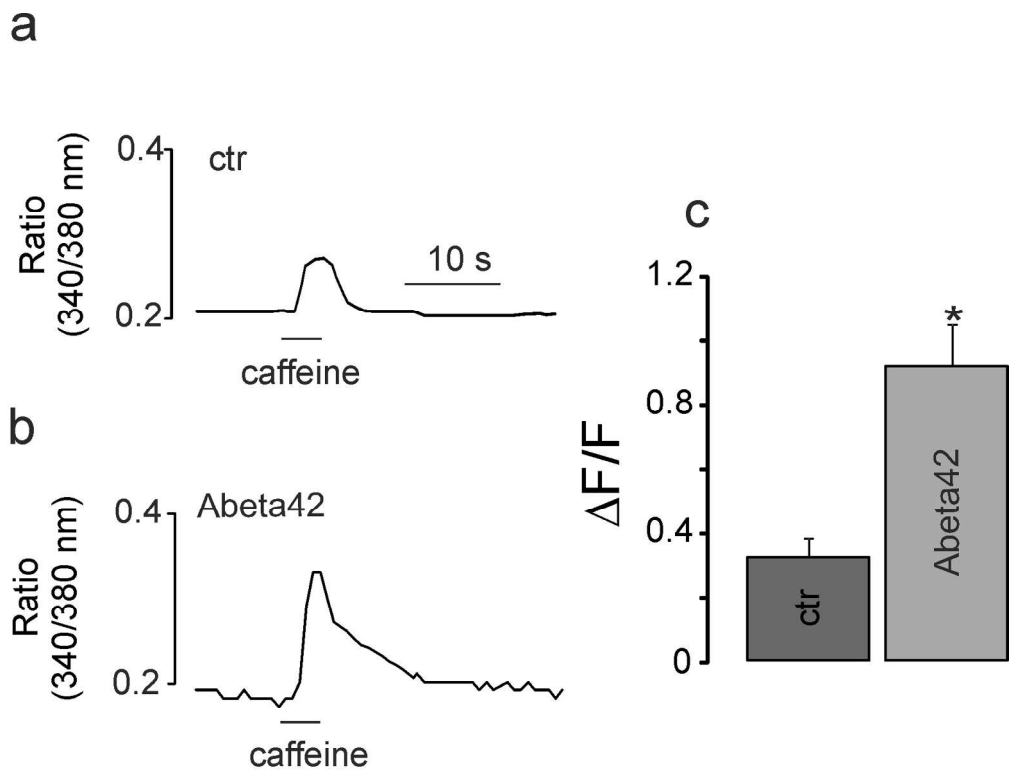

Fig. S2

Supplementary Figure S2

163x145mm (300 x 300 DPI)

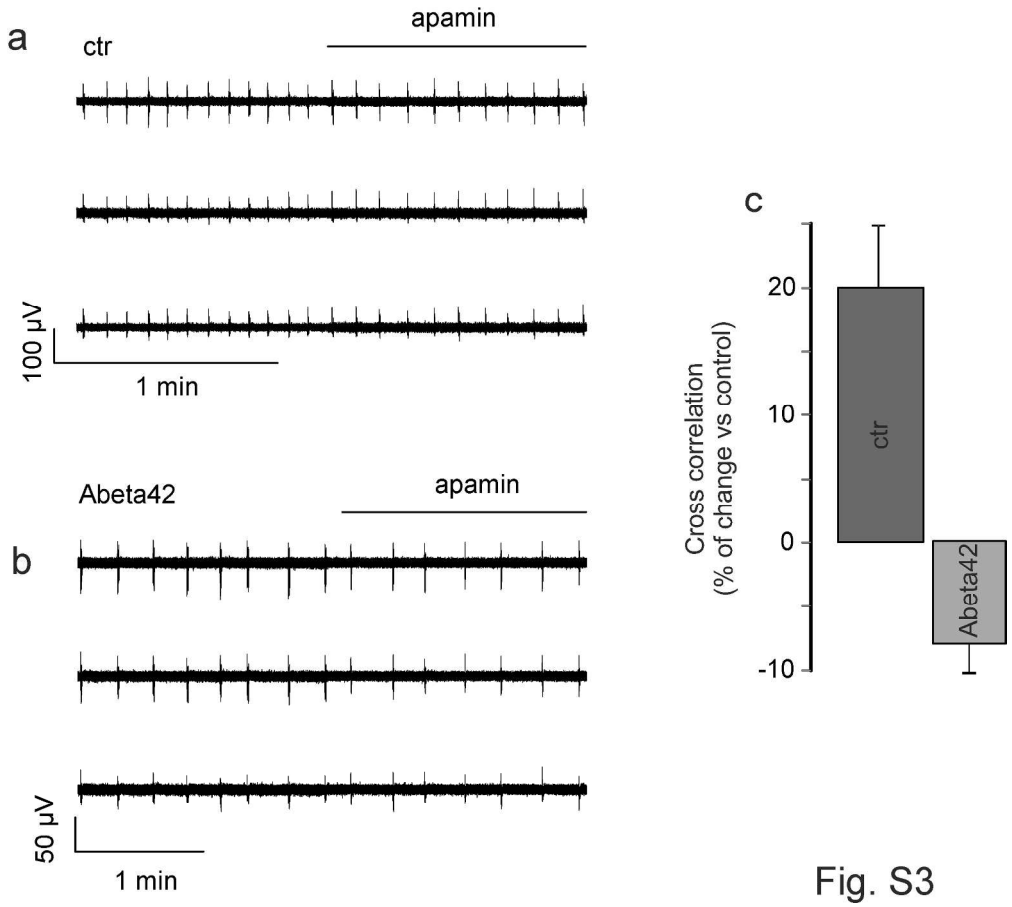

Fig. S3

Supplementary Figure S3

221x198mm (300 x 300 DPI)

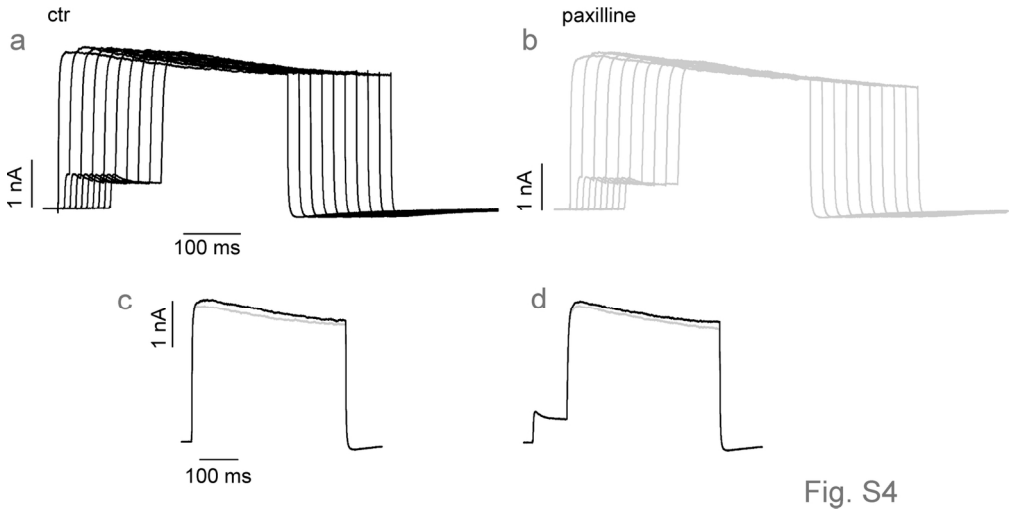

Fig. S4

Supplementary Figure S4

141x71mm (300 x 300 DPI)

Supplementary Fig. S1

a, b) 2x2μm AFM images of Abeta42 after 24h at 4°C (a: topography, b:phase signal) and (**c**, **d**) after 48h at 37°C (c: topography, d:phase signal). Height profile selected along two dotted lines (1, 2) are shown in (**a**) and (**c**).

Supplementary Fig. S2.

a) Effect of caffeine on intracellular Ca^{2+} concentration in control neurons. **b**) In neurons previously incubated with Abeta42 caffeine stimulates Ca^{2+} release as well. This effect is potentiated when compared to that observed in control neurons **c**) Bar graph summarizing the higher effect of caffeine on intracellular Ca^{2+} concentration in neurons treated with Abeta42 (light grey bar) with respect to control (dark grey bar).

Supplementary Fig. S3.

a) Three representative recording traces form the same MEA showing the lack of significant effect of SK channels block induced by apamin on spontaneous firing in control neurons. **b**) When apamin is added to neurons previously incubated with Abeta42 it decreases the spontaneous firing of hippocampal network. **c**) Bar graph summarizing the effect of apamin on network synchronization by measuring the crosscorrelation in control (dark grey bar) and in neurons incubated with Abeta42 (light grey bar). While apamin increases cross correlation in control neurons, the opposite is observed in the presence of Abeta42.

Supplementary Fig. S4.

(**a**) Voltage clamp recording of total outward K^+ current activated in control neurons by applying ten consecutive Ca^{2+} preloading stimuli at -10mV of increasing duration (from 0 ms to 90 ms) before depolarizing neurons to + 80 mV. **b**) BK channel contribution was estimated by administrating paxilline (1 µM). **c**, **d**) Overlapped traces from figure **a** (black traces) and **b** (gray traces) showing that the amount of BK channel activated current is similar when neurons are directly depolarized to + 80 mV (**c**) or preloaded with Ca^{2+} for 90 ms (**d**)